



**HAL**  
open science

## **Thermal remote sensing reveals communication between volcanoes of the Klyuchevskoy Volcanic Group**

Diego Coppola, Laiolo Marco, Francesco Massimetti, Sebastian Hainzl, Alina V Shevchenko, René Mania, Nikolai M. Shapiro, Thomas R Walter

► **To cite this version:**

Diego Coppola, Laiolo Marco, Francesco Massimetti, Sebastian Hainzl, Alina V Shevchenko, et al.. Thermal remote sensing reveals communication between volcanoes of the Klyuchevskoy Volcanic Group. Scientific Reports, 2021, 11, pp.13090. 10.1038/s41598-021-92542-z . hal-03291568

**HAL Id: hal-03291568**

**<https://hal.science/hal-03291568>**

Submitted on 19 Jul 2021

**HAL** is a multi-disciplinary open access archive for the deposit and dissemination of scientific research documents, whether they are published or not. The documents may come from teaching and research institutions in France or abroad, or from public or private research centers.

L'archive ouverte pluridisciplinaire **HAL**, est destinée au dépôt et à la diffusion de documents scientifiques de niveau recherche, publiés ou non, émanant des établissements d'enseignement et de recherche français ou étrangers, des laboratoires publics ou privés.

# 1 **The Kamchatka volcano orchestra – Remote sensing reveals communication** 2 **between volcanoes of the Klyuchevskoy Volcanic Group**

3

4 **Authors:** Diego Coppola<sup>1,2</sup>, Laiolo Marco<sup>1,2</sup>, Francesco Massimetti<sup>1,3</sup>, Sebastian Hainzl<sup>3</sup>, Alina V.  
5 Shevchenko<sup>3,4</sup>, Rene Mania<sup>3</sup>, Nikolai M., Shapiro<sup>5,6</sup>, Thomas R. Walter<sup>3</sup>

6

## 7 **Affiliations:**

8 (1) Dipartimento di Scienze della Terra, Università di Torino, Turin, Italy

9 (2) Centro Interdipartimentale sui Rischi Naturali in Ambiente Montano e Collinare, Università di Torino,  
10 Turin, Italy

11 (3) GFZ German Research Centre for Geosciences, Telegrafenberg, 14473 Potsdam, Germany

12 (4) Institute of Volcanology and Seismology FEB RAS, Piip boulevard 9, Petropavlovsk-Kamchatsky 683006,  
13 Russia

14 (5) Institut de Sciences de la Terre, Université Grenoble Alpes, CNRS (UMR5275), Grenoble, France

15 (6) Schmidt Institute of Physics of the Earth, Russian Academy of Sciences, Moscow, Russia

16

## 17 **Abstract**

18 Volcanoes are traditionally considered isolated with an activity that is mostly independent of the  
19 surrounding, with few eruptions only (<2%) associated with a tectonic earthquake trigger. Evidence is now  
20 increasing that volcanoes forming clusters of eruptive centers may simultaneously erupt, show unrest, or  
21 even shut-down activity. Using infrared satellite data, we detail 20 years of eruptive activity (2000-2020) at  
22 Klyuchevskoy, Bezymianny, and Tolbachik, the three active volcanoes of the Klyuchevskoy Volcanic Group  
23 (KVG), Kamchatka. We show that the neighbouring volcanoes exhibit multiple and reciprocal interactions on  
24 different timescales that unravel the magmatic system's complexity below the KVG. Klyuchevskoy and  
25 Bezymianny volcanoes show correlated activity with time-predictable and quasiperiodic behaviors,  
26 respectively. This is consistent with magma accumulation and discharge dynamics at both volcanoes, typical  
27 of steady-state volcanism. However, Tolbachik volcano can interrupt this steady-state regime and modify the  
28 magma output rate of its neighbors for several years. We suggest that below the KVG the transfer of magma  
29 at crustal level is modulated by the presence of three distinct but hydraulically connected plumbing systems.

30 Similar complex interactions may occur at other volcanic groups and must be considered to evaluate the  
31 hazard of grouped volcanoes.

32

### 33 **1. Introduction**

34 Closely located or clustered volcanoes may become conjointly active and are hence considered especially  
35 hazardous, yet robust evidence for their connectivity remains sparse. Examples of such a synchronized  
36 volcanic activity are discussed for neighboring volcanoes in Iceland<sup>1</sup>, Alaska<sup>2</sup>, Kamchatka<sup>3,4</sup>, Italy<sup>5</sup>, and  
37 elsewhere<sup>6,7</sup>, although larger time-scale synchronicity has been also reported for global volcanism<sup>8</sup>. Reasons  
38 for the linked activity of adjacent volcanoes are only poorly understood and may be locally different, including  
39 triggering by large tectonic earthquakes and associated stress changes within the crust<sup>9-14</sup>, and the  
40 competition of volcanoes for common reservoirs<sup>3,15</sup>. Conjoint unrest and deformation activity at clustered  
41 volcanoes occurs with temporal delays of days to months (or even more) and appears to be distance-  
42 dependent<sup>7</sup>. Magmatic sources spaced less than about 10 km apart tend to interact, whereas those spaced  
43 over 25 km do not<sup>7</sup>. However, interactions over longer distances (>20 km) have been hypothesized for  
44 volcanoes that share a common deep source, or in response to large dike intrusions or subduction  
45 earthquakes<sup>7</sup>. While observations suggest positively correlated feedback (one volcano triggers the other  
46 one), only a few examples<sup>5,16</sup> underline the existence of anti-correlated activity (i.e., volcanic unrest may shut  
47 down activity in the neighborhood).

48 Previous studies of correlated and anti-correlated volcanism are mainly based on poor data and reduced or  
49 biased eyewitness accounts. This is because reports often describe a singular, possibly sporadic occurrence  
50 of conjoint activity change, where eruptions are more likely to be reported than periods of quiescence and  
51 decreasing activity. Robust and statistically significant testing of repeat observations was not yet achieved  
52 and may overcome some of the reporting limitations.

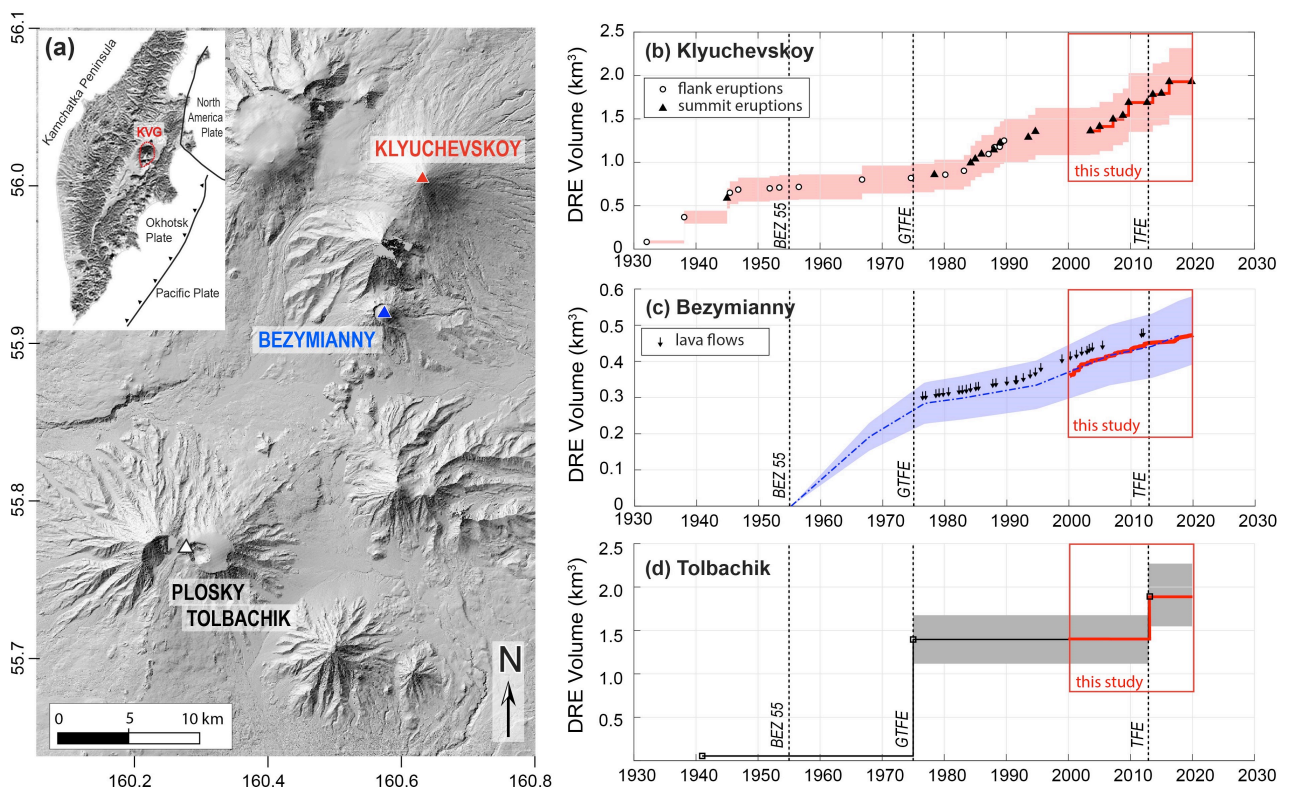
53 Here we employed a unique time-series of satellite thermal data (from 2000 to 2020) derived from the  
54 Moderate Resolution Imaging Spectroradiometer (MODIS) sensor<sup>17</sup>, to study potential volcano interactions  
55 within the Klyuchevskoy Volcano Group (KVG) in Kamchatka (Russia). The KVG hosts three adjacent (~10 to  
56 30 km distant) active volcanoes (Klyuchevskoy, Bezymianny, and Tolbachik), with contrasting eruptive  
57 products that possibly indicate different magmatic sources and a compound multilevel feeding system<sup>18,19</sup>.  
58 Whether this composite feeding system forms a single interconnected trans-crustal magmatic system<sup>20</sup>, and  
59 in which degree the three volcanoes interact remains so far an open question<sup>21,22</sup>.

60 The Klyuchevskoy Volcanic Group (KVG) has been monitored for >50 years by the Kamchatkan Branch of the  
61 Geophysical Survey of the Russian Academy of Sciences (KBGS). Due to harsh climate conditions, the  
62 monitoring system mainly consists of seismic stations and webcams. Nowadays, 17 telemetric stations

63 transmit the data to the central monitoring office, where it is being analyzed in real-time<sup>23</sup> and allowed to  
 64 investigate the deep structure of KVG<sup>24</sup>. Although localized and dense seismic networks were installed for  
 65 short-term times<sup>25,26</sup>, these experimental networks do not permit decade-long analysis and robust statistics,  
 66 so that details on eruption occurrence and eruption rates remained hidden. As this work shows, satellite  
 67 thermal remote sensing reveals complex interactions under the KVG, whereby each volcano is able to  
 68 influence its neighbors. Distinct eruptive activity appears sometimes in chorus and sometimes separate,  
 69 comparable to an orchestra.

70

71



72

73 **Figure 1.** (a) Distribution of volcanic centers within the Klyuchevskoy Volcanic Group (KVG). Right panels show  
 74 the Cumulative Dense Rock Equivalent (DRE) volumes of lavas erupted between 1930 and 2020 for (b)  
 75 Klyuchevskoy<sup>21</sup>, (c) Bezymianny<sup>44</sup>, and (d) Tolbachik<sup>57</sup>. All volumes are recalculated for DRE using: (i) a magma  
 76 density of  $2800 \text{ kg m}^{-3}$  and an average density of lava flows of  $2500 \text{ kg m}^{-3}$  for Klyuchevskoy and Tolbachik<sup>57</sup>;  
 77 (ii) a magma density of  $2500 \text{ kg m}^{-3}$  and an average density of lava dome of  $2000 \text{ kg m}^{-3}$  for Bezymianny<sup>41</sup>. A  
 78 standard error of  $\pm 20\%$  (colored fields) takes into account uncertainties in the estimates of bulk volumes and  
 79 densities of erupted products. Red bold lines within insets, correspond to satellite-derived volumes (this  
 80 work; see Methods). The grey bars outline the timing of the Bezymianny eruption in 1955-56 (BEZ55), the  
 81 Great Tolbachik Fissure Eruption in 1975 (GTFE) and the Tolbachik Fissure Eruption in 2012 (TFE). Shaded  
 82 relief map derived from ArcticDEM digital elevation model (<https://www.pgc.umn.edu/data/arcticdem/>)  
 83 and elaborated using QGIS version 3.16.3 (<http://qgis.osgeo.org/>); Time series generated using MATLAB software  
 84 ([www.mathworks.com](http://www.mathworks.com)).

85

86

87

**88 2. The Klyuchevskoy Volcanic Group (KVG)**

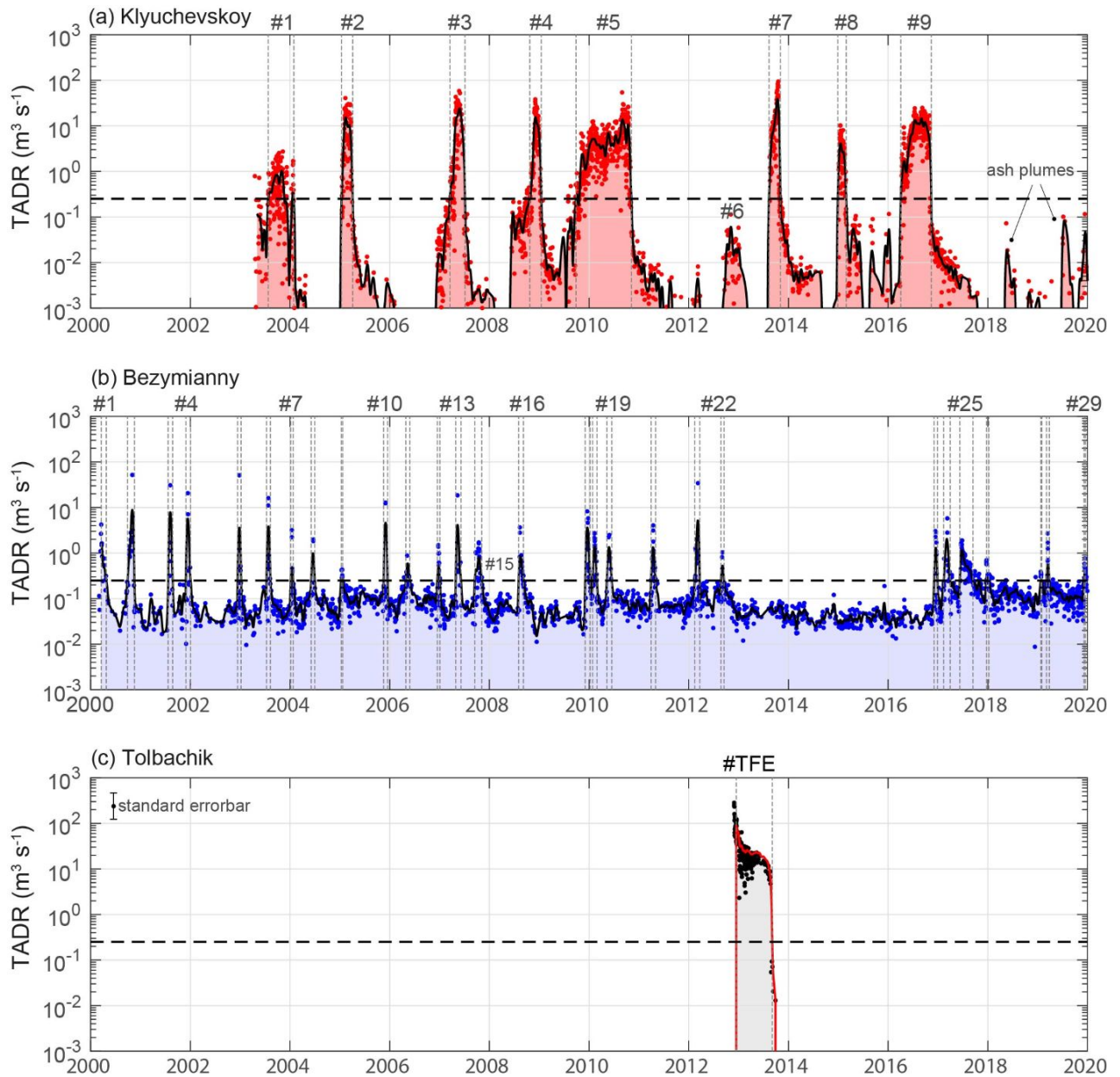
89 The KVG is a prominent volcanic massif located in the northern part of the Central Kamchatka Depression.  
90 Dozens of volcanic centers were built during the construction of the massif, which currently has three active  
91 volcanoes: Klyuchevskoy, Bezymianny, and Tolbachik (Fig. 1a). The KVG is a very active and relatively young  
92 volcanic massif mainly developed during the last 300–400 ka<sup>27</sup>. Volcanism is fed by sub-arc mantle, melted  
93 under an influx of melts and fluids from the subducting Pacific plate<sup>28-32</sup>. Additional influx of hot mantle  
94 following recent slab detachment<sup>33</sup>, and interaction with metasomatized mantle<sup>34,35</sup> contribute to the  
95 exceptional level of volcanic activity in the area and the very diverse volcanic manifestations and products.  
96 Seismic activity of the KVG volcanoes is abundant and includes long periods of sustained tremors as well as  
97 numerous volcano-tectonic (VT) and long-period (LP) events. The latter mostly occur at two depth ranges:  
98 above 5 km and close to 30 km<sup>22</sup>. Geophysical and petrographic data have been used to infer that all the KVG  
99 volcanoes are fed by a common parental magma<sup>36</sup>. However, different isotope compositions of rocks from  
100 Klyuchevskoy and Bezymianny<sup>19,34</sup> do not support such view, in favor of multiple magma sources, with only  
101 limited interaction.

102 Klyuchevskoy volcano (4750 m a.s.l.) is the highest in the group and one of the world's most active volcanoes.  
103 Its recent activity is characterized by the effusion of voluminous basaltic andesite lava flows, often associated  
104 with moderate to violent explosive activity. Between 1930 and 2005, the volcano has erupted an estimated  
105  $\sim 1.5 \times 10^9$  m<sup>3</sup> of lava<sup>37</sup> (dense rock equivalent; DRE), with an average magma output rate (DRE) of  $\sim 0.67$  m<sup>3</sup>  
106 s<sup>-1</sup>. The output rate accelerated since 1978, associated with a change in the eruptive pattern that shifted from  
107 flank- to summit-dominated eruptions<sup>37</sup> (Fig.1b). After nine years of rest, in 2003, the volcano began a new  
108 activity phase characterized by nine summit eruptions until December 2019<sup>38</sup>. Seismic, geodetic, and  
109 petrographic data<sup>18,21,22,25,37</sup> suggest that Klyuchevskoy's eruptions are fed through a sub-vertical, pipe-like  
110 conduit extending to a depth of 30-50 km below the volcano, where the primary magma reservoir is located.  
111 On its way to the surface, the magma is stored at a depth of 15-25 km and then transported further upwards  
112 to a shallow (3-5 km deep) peripheral reservoir<sup>24</sup>. During ascent, the magma evolves from high-Mg low-Al  
113 basalt to low-Mg high-Al basaltic andesite<sup>39</sup>, making it different from the eruptive products of the other active  
114 KVG volcanoes<sup>36</sup>. Eventually, before the conduit reaches the summit crater, numerous radial dikes depart  
115 and feed eruptions at the mid- and lower-volcano flanks<sup>21,37</sup>.

116 Bezymianny is an andesitic volcano (2,882 m a.s.l.) that reawakened in 1955-56 with a paroxysmal eruption  
117 (VEI 5) that disrupted the old cone forming a large horseshoe-shaped crater<sup>40</sup>. Since then, near-continuous  
118 lava dome growth was accompanied by mostly explosive activity<sup>41,42</sup>. The greatest rate of dome growth

119 occurred during the first two decades until 1977 (Fig. 1c), when lava flows were observed for the first time  
120 marking a pivotal change in the volcano's dome growth mechanism<sup>42-44</sup>. Ever since then, Bezymianny's  
121 eruptions showed a recurrent cyclical behavior depicted by extrusive-explosive-effusive activity<sup>41,42</sup>. Previous  
122 works<sup>45-49</sup> outlined how this cyclic activity was accompanied by precursory thermal radiation preceding the  
123 explosive events by few weeks to days. Until 2017, more than 55 distinct episodes of dome-growth filled  
124 most of the 1956 collapse amphitheater<sup>38,42</sup> gradually developing a stratocone with an average growth rate<sup>44</sup>  
125 of  $\sim 0.30 \text{ m}^3 \text{ s}^{-1}$  (blue line in Fig. 1c). Geophysical and petrological data suggest a multi-level magma plumbing  
126 system beneath Bezymianny volcano with at least three crustal reservoirs located between 10-18 km, 5-8  
127 km, and  $< 2$  km depth<sup>18,26,50-54</sup>.

128 The Tolbachik massif comprises two large stratocones, Ostry ("Sharp") Tolbachik (3682 m a.s.l.) and Plosky  
129 ("Flat") Tolbachik (3085 m a.s.l.), in the southernmost part of the KVG<sup>55</sup> at approximately 30 km distance to  
130 Kluchevskoy and  $\sim 20$  km distance to Bezymianny (Fig. 1a). A 70 km long zone of monogenetic basaltic cones  
131 extends across the Plosky Tolbachik cone; whose southern branch was the place of the 1975-1976 Great  
132 Tolbachik Fissure Eruption (GTFE)<sup>56</sup>. This eruption produced extensive lava fields composed of high-  
133 magnesium and high-aluminum basalts, from northern and southern vents, respectively<sup>55</sup>. With a total DRE  
134 volume of  $\sim 1.5 \times 10^9 \text{ m}^3$  (Fig. 1d), it was one of the largest basaltic eruptions in Kamchatka during historical  
135 times<sup>56</sup>. After the GTFE, no signs of activity were recorded until November 2012, when increased seismic  
136 activity heralded the beginning of a new eruption<sup>57</sup>. The 2012-2013 eruption took place at the south flank of  
137 the Plosky Tolbachik cone and was dominated by Hawaiian-style activity associated with an emplacement of  
138 a large lava field<sup>58</sup>. During the 205 days of activity, a lava volume of  $\sim 0.5 \times 10^9 \text{ m}^3$  was erupted, with a gently  
139 declining trend throughout the whole eruptive period<sup>58</sup>. Satellite geodesy could reveal the intrusion of a 6.1  
140 km long dike intrusion, opening up to 8 m, adding almost 10% to the total eruption volume<sup>59</sup>. The activity  
141 ceased entirely by the end of August 2013. According to Koulakov et al.<sup>18</sup>, one magmatic pathway of Tolbachik  
142 appears to be connected with the marginal part of the Klyuchevskoy deep reservoir, and another seems to  
143 originate from an independent mantle source located to the south of Tolbachik.



144

145 **Figure 2** – Time-series of the Time-Averaged lava Discharge Rate (TADR; logarithmic scale) for (a)  
 146 Klyuchevskoy, (b) Bezymianny, and (c) Tolbachik. Single satellite measurements (dots) are interpolated and  
 147 smoothed (line) to provide continuous data. The horizontal dashed lines represent the threshold of  $0.25 \text{ m}^3$   
 148  $\text{s}^{-1}$  used for automatized detection of eruptions (see Methods section). The start and end of each eruptive  
 149 period (labelled on the top of each plot) are marked by the vertical dashed lines. The error for every single  
 150 datapoint is  $\pm 50\%$ . The time series is generated using MATLAB software ([www.mathworks.com](http://www.mathworks.com)).

151

152

### 153 3. Remote sensing of eruption effusion rates

154 We calculated the Time-Averaged lava Discharge Rate (TADR) and the erupted lava volumes at the three  
 155 volcanoes by using MODIS infrared data acquired between March 2000 and December 2019 (bold lines in  
 156 insets of Fig. 1b,c,d) determined with the MIROVA system<sup>17,60</sup>. Details of the methodology and associated

157 limits are described in the *Methods* section accompanying this paper. A TADR threshold of  $0.25 \text{ m}^3 \text{ s}^{-1}$  is used  
158 to automatically recognize the main eruptive periods at each volcano (Fig. 2), and to quantify the eruption  
159 parameters summarized in Table 1.

### 160 **3.1. Klyuchevskoy**

161 Nine eruptions occurred at Klyuchevskoy between 2003 and 2020 (Fig.2a). Of these, eight were automatically  
162 recognized (see Methods), and one was manually selected, based on observations of Ozerov et al.<sup>38</sup> (eruption  
163 #6; Table 1). Most of the eruptions (#2,3,4,5,7,8,9; Table 1a) produced lava flows along the flanks of the  
164 volcano<sup>38</sup> and created lava volumes ranging from  $\sim 10$  to  $150 \times 10^6 \text{ m}^3$  each, with a Mean Output Rate (MOR:  
165 total volume of eruption/duration) ranging between 2.5 and  $10 \text{ m}^3 \text{ s}^{-1}$  and a maximum TADR often higher  
166 than  $30 \text{ m}^3 \text{ s}^{-1}$  (Table 1a). Only two eruptions (#1,6; Table 1a) were limited to moderate explosive activity  
167 inside the summit crater<sup>38</sup> characterized by much lower volumetric output ( $< 10 \text{ Mm}^3$ ) and discharge rates  
168 (maximum TADR  $< 2.5 \text{ m}^3 \text{ s}^{-1}$ ; Table 1a). For some eruptions (#3,4,5; Fig. 2a), the onset of lava effusion was  
169 preceded by a precursory phase of several weeks, identified by increased fumarolic activity and degassing<sup>38</sup>.  
170 In other cases, the beginning of the eruption was rather rapid, without any apparent thermal precursory  
171 phase (#2,7,8,9; Fig. 2a). The eruptive trends of Klyuchevskoy are often characterized by a TADR that  
172 increases with time to reach values of  $10\text{-}100 \text{ m}^3 \text{ s}^{-1}$  immediately before the effusion suddenly ceases (Fig.  
173 2a). The volumetric output of the 20 years (Fig. 2) defines the most recent period of intense activity of  
174 Klyuchevskoy characterized by a steady-state output rate ( $Q_{ss}$ ) of  $1.36 \text{ m}^3 \text{ s}^{-1}$  ( $1.21 \text{ m}^3 \text{ s}^{-1}$  DRE; Fig 3a), which  
175 is almost twice the average output since 1930 (Fig. 1b1). Notably, the cumulative curve in Fig. 3a shows a  
176 clear sawtooth pattern typical for steady-state volcanism<sup>61</sup> whereby each step is either produced by (i) an  
177 unbuffered arrival and eruption of discrete magma batches, or (ii) a partial or complete discharge of a shallow  
178 reservoir that is fed by a constant magma supply. A similar pattern could be also explained if the arrival of  
179 discrete magma batches is controlled by a steady-state destabilization of magma reservoirs, produced by  
180 passive degassing during quiescence, which can trigger magma ascent from depth<sup>62-64</sup>. Whatever the model,  
181 the two lines, which envelope the sawtooth curve (parallel to the linear trend  $\pm 2\sigma$ ; Fig. 3a), define the  
182 maximum size (maximum eruptible lava volume) and maximum response time of the individual eruption,  
183 respectively<sup>61</sup>. For Klyuchevskoy, these values are approximately  $143 \times 10^6 \text{ m}^3$  and 1214 days. The analysis of  
184 inter-eruption time distribution (*Methods*) suggests a relatively strong periodicity (Fig. 4a). The degree of  
185 periodicity can be quantified by the coefficient of variation (CV), which is zero for perfect periodicity, one for  
186 randomness, and larger than one for clustering. In the case of Klyuchevskoy's eruptions, we found a CV equal  
187 to 0.38 and the inter-eruption time positively correlated to the size of the last event (correlation coefficient  
188 of 0.65), as expected for time-predictable systems (Fig. 4a). A load and discharge model is thus envisaged for  
189 Klyuchevskoy (Fig. 3), whereby an eruption starts when the upper, critical volume threshold is accumulated  
190 in the shallow reservoir<sup>65</sup>. The resumption of eruptive activity on November 2019<sup>66</sup> further supports a time-

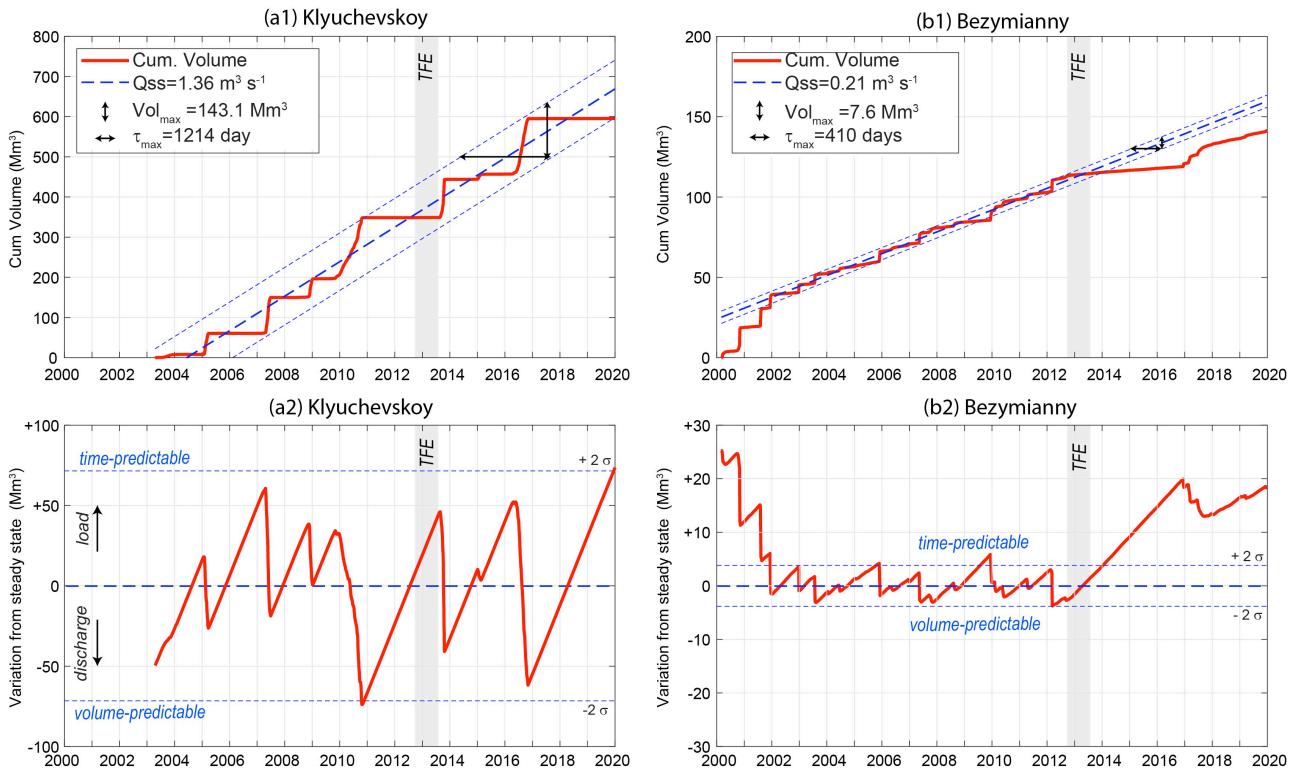


191 predictable behavior (*Methods*), which is in agreement with the achievement of a critical volume as shown  
192 in Fig. 3a.

193

### 194 **3.2. Bezymianny**

195 Thermal data acquired over Bezymianny (Fig. 2b) are indicative of an open-vent volcano, persistently emitting  
196 hot volcanic products. The retrieved long-term eruptive pattern can be subdivided into two distinct regimes:  
197 (1) a continuous low-level regime, associated with passive degassing and possibly related to “endogenous  
198 growth,” and (2) an intermittent high-level regime, associated with short-term (days to weeks) extrusive-  
199 explosive-effusive cycles. A TADR threshold of  $0.25 \text{ m}^3 \text{ s}^{-1}$  separates the two regimes and automatically  
200 recognizes 28 out of the 29 major eruptive cycles between 2000 and 2019<sup>38,42</sup> (Table 1b). The only undetected  
201 event occurred on 5 November 2007, when strong cloud coverage over the volcano prevented the detection  
202 of this short-lived event (Table 1). Each eruption cycle is characterized by erupted volumes ranging from  
203  $\sim 0.15$  to  $\sim 15 \times 10^6 \text{ m}^3$  and peak TADRs between  $0.35$  to  $52 \text{ m}^3 \text{ s}^{-1}$  (Table 1b). The average duration of each  
204 eruptive cycle is  $26.7 (\pm 20.7; 1\sigma)$  days, much shorter than the average inter-eruption time of 222.7 days. The  
205 cumulative volume curve of Bezymianny is essentially controlled by the sudden steps associated with the  
206 eruptive cycles detected by MODIS (Fig. 3c). Between 2000 and mid-2002, eruptions reached higher TADR  
207 peaks, causing a steeper cumulative volume curve than in the rest of the time series (Fig. 3c). Although this  
208 may reflect a higher magma output rate in this period, it is also possible that the dataset is biased by the fact  
209 that only one satellite was operating in that period (see *Methods*). Similar to Klyuchevskoy, the cumulative  
210 curve of the volumes erupted between May 2002 and September 2012 suggests steady-state volcanism for  
211 Bezymianny<sup>61</sup>, which is characterized by an average output rate of  $\sim 0.21 \text{ m}^3 \text{ s}^{-1}$ , a maximum eruptible volume  
212 of  $\sim 7.6 \times 10^6 \text{ m}^3$ , and a maximum repose time of 410 days (Fig. 3c and 3d). A notable lack of eruptive cycles  
213 occurred between September 2012 and December 2016 (Fig. 2b). This anomalously long rest period (low  
214 thermal regime) is also visible in Fig. 3b and 3c, where the cumulative volume curve diverges horizontally  
215 from the steady-state model. According to Wadge<sup>61</sup>, this pattern occurs at steady-state volcanoes when  
216 magma is not being supplied into the shallow reservoir, here either because magma is not being generated  
217 or a neighboring volcano is capturing it. Bezymianny's activity resumed at the end of 2016 and continued  
218 intermittently with an output rate similar to the 2002-2012 period. The analysis of inter-eruption times  
219 (*Methods*) suggests a quasi-periodic behavior ( $CV=0.5$ ) for Bezymianny's activity until 2012 (Fig. 4b), which is  
220 completely lost when including the whole dataset (Fig. 4c). No correlation is found between the inter-  
221 eruption times and volumes released during the last or the next eruption (Fig. 4). Although the lack of  
222 correlation can be due to the significant uncertainties affecting the Bezymianny time series (*Methods*), we  
223 may not exclude the role of a time-varying upper threshold (strength) of the shallow magmatic system<sup>65</sup>.



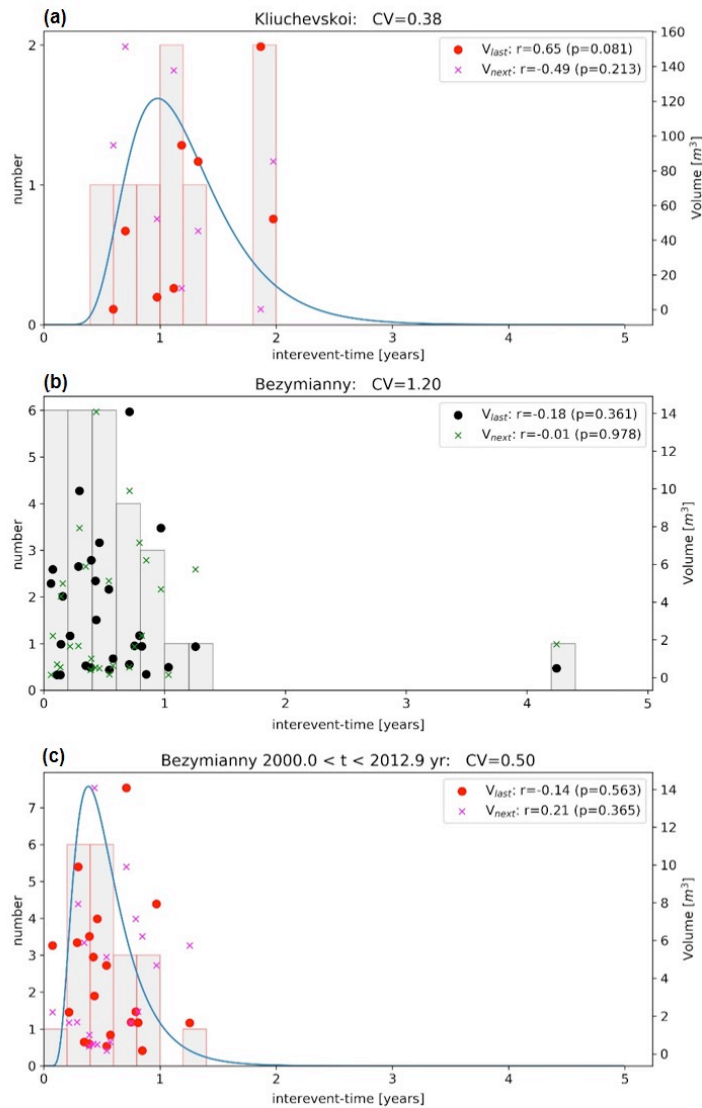
224

225 **Figure 3 – Upper panels.** Cumulative volume curves for (a1) Klyuchevskoy and (b1) Bezymianny, derived from  
 226 satellite measurements (see Methods). The linear fits of each cumulative curve represent the linear growth  
 227 model (blue thick dashed lines) and provide the steady-state output rate (Q<sub>ss</sub>). The two parallel lines (linear  
 228 model ± 2σ) define the maximum eruptible volume (Vol<sub>max</sub>) and the maximum response time (τ<sub>max</sub>) for the  
 229 inferred steady-state condition. **Lower panels.** Load and discharge model for (a2) Klyuchevskoy and (b2)  
 230 Bezymianny. The variation from the steady-state is calculated as the residual between the linear growth  
 231 model and the observed cumulative volume curves. A two-fold standard deviation (± 2σ) of residual is used  
 232 to define the upper and lower volume limits for the load-discharge model. In this plot, a time-predictable  
 233 system would have a near-constant upper threshold of the volume load when eruptions occur. A volume-  
 234 predictable system would have a near-constant lower threshold. An entirely predictable system would have  
 235 both. The gray bar indicates the timing of the 2012 Tolbachik Fissure Eruption (TFE). Time series generated  
 236 using MATLAB software ([www.mathworks.com](http://www.mathworks.com)).

237

### 238 3.3 Tolbachik

239 The eruption of Tolbachik (November 2012 – August 2013) commenced suddenly on 27 November 2012,  
 240 producing an initial TADR peak of about 300 m<sup>3</sup> s<sup>-1</sup>. This initial activity resulted in the emplacement of a lava  
 241 flow that reached a length of about 15 km in a few days<sup>67</sup>. Effusion rates decrease roughly exponentially  
 242 during the following ten months of continuous effusive activity. The eruption stopped between 23 and 27  
 243 August 2013 when the TADR suddenly lowered from 7-9 to less than 0.25 m<sup>3</sup> s<sup>-1</sup>. The eruption emplaced a  
 244 volume of ~0.5 × 10<sup>6</sup> m<sup>3</sup> in 302 days<sup>58</sup>, which is up to 4000 times the volume commonly erupted at  
 245 Bezymianny volcano (>0.15 × 10<sup>6</sup> m<sup>3</sup>, see above).



246

247 **Figure 4** - Inter-eruption times distribution (bars) for (a) Klyuchevskoy, (b) Bezymianny - whole period (2000-  
 248 2020), (c) Bezymianny - pre-Tolbachik eruption (2000-2012). The coefficient of variation (CV), a measure for  
 249 the eruption's periodicity, is provided in the title of each plot. Symbols show the eruption volume (right axis)  
 250 in all three panels as a function of the inter-eruption time, where points and crosses refer to the volume of  
 251 the last and next event, respectively. The correlation coefficient ( $r$ ) between volume and interevent-time  
 252 with its  $p$ -value is provided in the legends.  
 253

254 **4. Interactions between Klyuchevskoy, Bezymianny, and Tolbachik**

255 We statistically explore if the three volcanoes interacted on more than one occasion and in different ways.  
 256 Specifically, we found various degrees of interactions that become best observable by analyzing the data at  
 257 the time scales from weeks to decades.

258 Below we provide evidence of interactions related to (i) conjoint activity of Klyuchevskoy and Bezymianny  
 259 throughout 2003-2020, (ii) the reactivation of Tolbachik in 2011-2012, (iii) the reactivation of Klyuchevskoy  
 260 and the cessation of Tolbachik in August 2013, (iv) the reactivation of Bezymianny in 2016-2017, and (v)

261 changes in the long-term magma output rate after the Bezymianny eruption, in 1955-56, and after the Great  
262 Tolbachik Fissure Eruption (GFTE), in 1977.

263

#### 264 **4.1. Conjoint activity and pattern's change before and after the 2012 Tolbachik eruption**

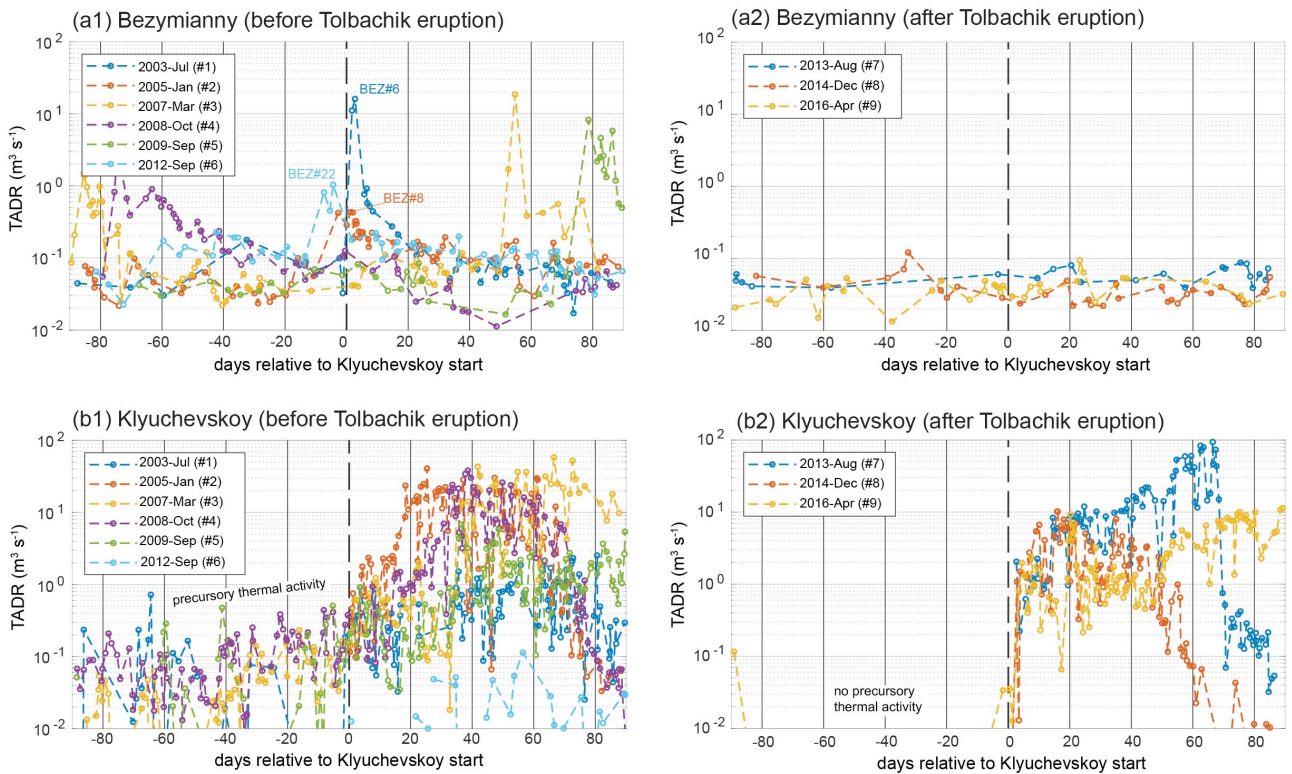
265 A first indication of how volcanoes are interconnected with each other is revealed by the detailed analysis of  
266 the mutual activity of Klyuchevskoy and Bezymianny (and pattern's change) before and after the Tolbachik  
267 eruption (Fig. 5).

268 Before the latter (Fig. 5a1), we observe a simultaneous activation of Bezymianny and Klyuchevskoy several  
269 times (i.e., eruptions KLY#1,2,6) while no simultaneous activation is found afterward (Fig. 5a2). In particular,  
270 the onset of Klyuchevskoy's eruptions #1,2,6 coincided with the maximum activity of Bezymianny  
271 (BEZ#6,8,22) in the same period (a time window of  $\pm 10$  days is considered to avoid the effect of clouds).  
272 Although less significant, Bezymianny's activity also showed some synchronous activation (increase of TADR  
273 relative to the previous trend) with the onset of the other Klyuchevskoy eruptions (KLI#3,4) before the  
274 Tolbachick eruption.

275 More specifically, we found that in the days-to-weeks following each of Klyuchevskoy eruptions, the average  
276 TADR of Bezymianny increased, on average, by a factor of four (*Methods*). This increase suggests that before  
277 2012, the eruptions of Klyuchevskoy were able to “galvanize” also the activity of Bezymianny. In contrast,  
278 after the eruption of Tolbachik, the two volcanoes no longer have erupted simultaneously.

279 Additionally, before the Tolbachik eruption, most of the eruptions of Klyuchevskoy were characterized by a  
280 precursory phase marked by a gradual increase in thermal activity and estimated TADR (Fig. 5b1). This pre-  
281 eruptive pattern is typical of open-vent volcanoes, in which the rise of the magma column causes the  
282 appearance and growth of fumaroles or weak explosive activity<sup>68</sup>. However, the precursory pattern  
283 disappeared after the eruption of Tolbachik (Fig. 5b2), and all the three subsequent eruptions of  
284 Klyuchevskoy showed a sudden beginning of activity more typical of closed-vent systems<sup>68</sup>.

285



286  
287

288 **Figure 5** - Stacked TADR time-series relative to the onset of the Klyuchevskoy eruptions, before (left column)  
 289 and after (right column) the Tolbachik eruption. **Upper panels:** TADRs of the Bezymianny volcano. **Lower**  
 290 **panels:** TADRs of the Klyuchevskoy volcano. The simultaneous activation of Bezymianny at the time of the  
 291 eruption onset of Klyuchevskoy is obvious before the Tolbachik eruption (a1) but absent afterwards (a2).  
 292 Similarly, at Klyuchevskoy, the precursory activity is evident for the eruptions that occurred before the  
 293 Tolbachik eruptions (b1), but not afterward (b2). Time series generated using MATLAB software  
 294 ([www.mathworks.com](http://www.mathworks.com)).

295

296

#### 297 **4.2. Reactivation of Tolbachik in 2011-2012**

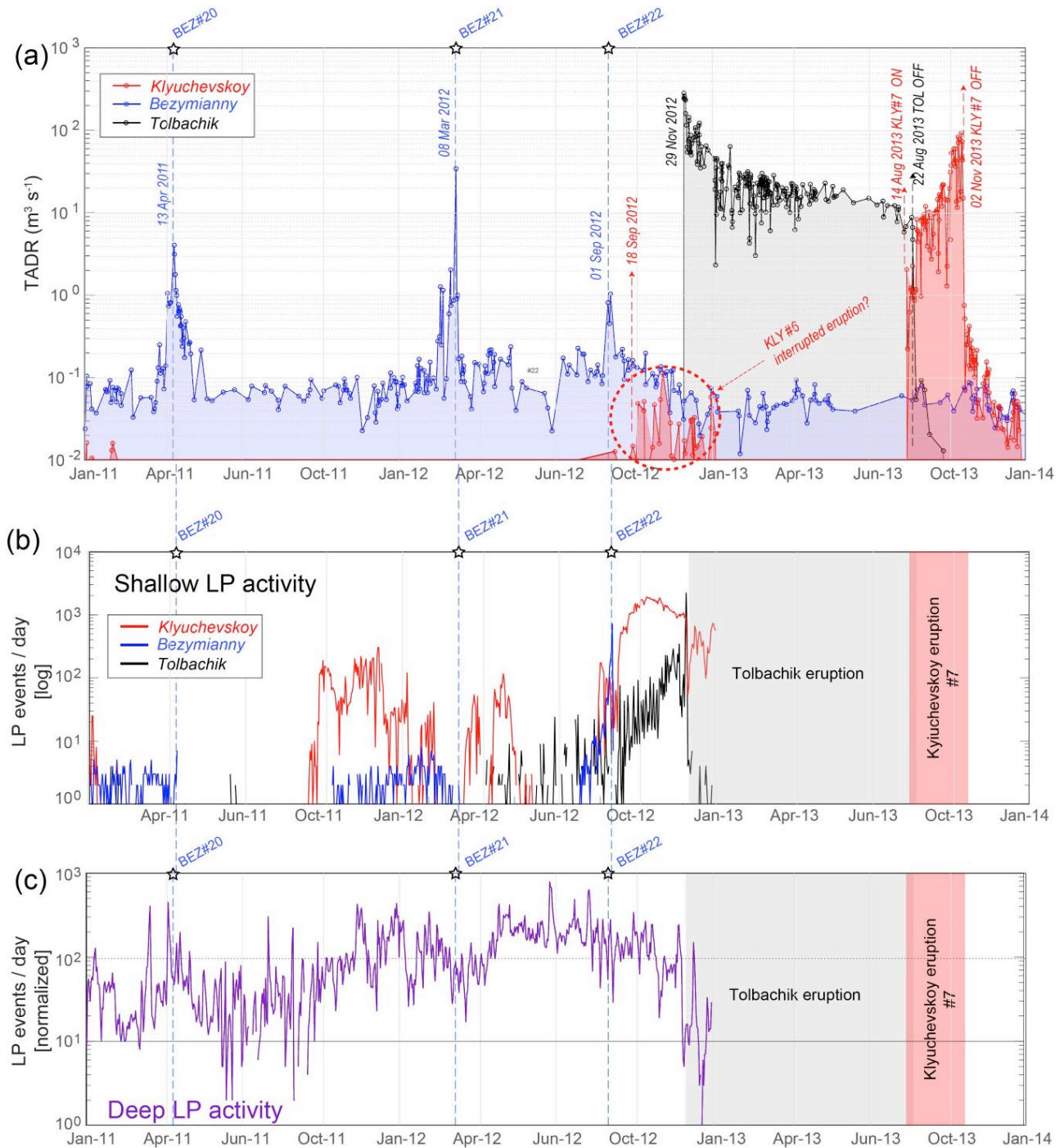
298 The comparison between the surface activity, retrieved from satellite, and the long-period (LP) earthquakes  
 299 occurred within the KVG during the reactivation of Tolbachik<sup>22,70</sup>, provides further indications of mutual  
 300 communication between these volcanoes. This last was preceded in 2011 by an increase of the Deep Long  
 301 Period (DLP) seismic activity reaching its maximum level in May 2012 (Fig. 6c). It reflected the gradual  
 302 pressurization of the whole KVG plumbing system<sup>70</sup>, possibly in response to a pulse of volatile-rich basaltic  
 303 magmas rising from the mantle<sup>71</sup>. At Bezymianny, this gradual pressurization may have triggered three  
 304 consecutive shallow LP swarms, each preceding an eruption, the last one being in September 2012 (Fig. 6a,b).  
 305 Similarly, LP seismicity also migrated shallow below the Klyuchevskoy volcano in September 2012 (promptly  
 306 triggering the onset of eruption #6), and later, on October-November 2012, LPs occurred below Tolbachik,  
 307 just before the onset of its voluminous flank eruption (Fig. 6a,b).

308 Interestingly, during eruption #6 of Klyuchevskoy, the TADR trend almost mirrors the shallow LP seismicity,  
 309 both reaching a maximum in November 2012 and then declining in correspondence with an acceleration of

310 the Tolbachik seismic swarm (Fig. 6a,b). Eruption #6 was somehow unusual for Klyuchevskoy since it  
311 produced only weak Strombolian activity<sup>38</sup>, with a TADR always below  $0.25 \text{ m}^3 \text{ s}^{-1}$  and a volume of less than  
312  $1 \times 10^6 \text{ m}^3$  (Table 1). Moreover, unlike the other Klyuchevskoy eruptions (cf. Fig. 2a), it never culminated in  
313 effusive activity, which is atypical for this volcano. Together with a waning trend of surface and seismic  
314 activity since mid-November 2012, these peculiar features suggest a sort of partial depletion of the shallow  
315 magma supply of Klyuchevskoy, precisely in correspondence with the acceleration of seismic swarms below  
316 Tolbachik (Fig. 6a,b). It is worth noting that the eruptions of Klyuchevskoy stopped in 1975–1976 during the  
317 GFTE and were renewed in 1977–1978 after the GFTE<sup>72</sup>.

318

319



320

321 **Figure 6** Reactivation of Tolbachik and responses at other volcanoes. – (a) Stacked TADR time-series for  
 322 Klyuchevskoy, Bezymianny, and Tolbachik between 2011 and 2014. (b) Shallow LP seismicity (normalized  
 323 number of events per day) below the Klyuchevskoy, Bezymianny, and Tolbachik during the same period  
 324 (modified from Shapiro et al., 2017); (c) Deep LP seismicity below the KVG (seismic data modified from  
 325 Shapiro et al., 2017); (refer to the color version of the figure). Time series generated using MATLAB software  
 326 (www.mathworks.com).

327

### 328 **4.3. Reactivation of Klyuchevskoy and cessation of Tolbachik eruption in August 2013**

329 Even more intriguing is the resumption of the activity at Klyuchevskoy (eruption #7) and the almost  
 330 concurrent cessation of activity at Tolbachik on 22 August 2013 (Fig. 6a). The beginning of eruption #7

331 occurred suddenly on 14 August 2013, with the onset of Strombolian explosions, which evolved in few days  
332 into summit effusive activity<sup>38</sup> fed with a TADR of about  $10 \text{ m}^3 \text{ s}^{-1}$  (Fig. 6a). Lava discharge rates increased  
333 rapidly in the following months to reach a maximum value of  $\sim 100 \text{ m}^3 \text{ s}^{-1}$  on 18 October 2013, just before the  
334 abrupt cessation of surface activity on 25 October 2013.

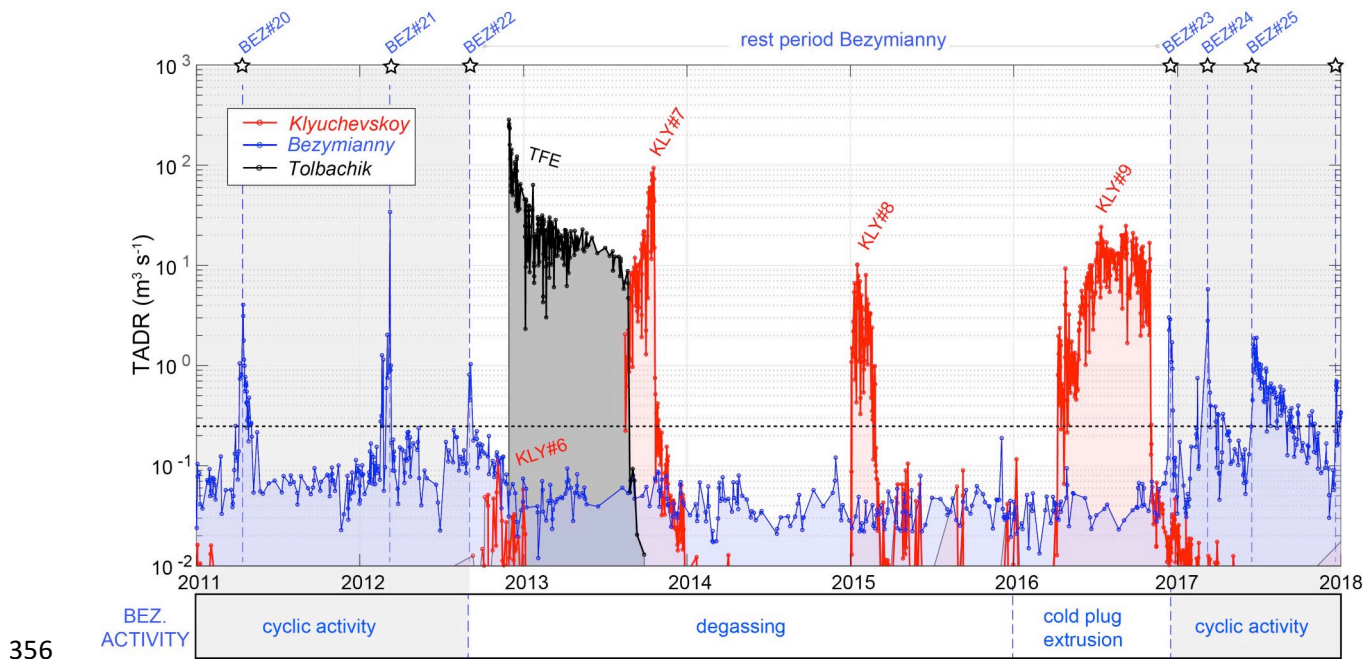
335 The onset of eruption #7, which also occurred abruptly on 14 August 2013, preceded the end of the Tolbachik  
336 eruption by eight days (Fig.6a). Our data suggest that the Tolbachik eruption ended when the TADR-values  
337 were still moderately high ( $7\text{-}9 \text{ m}^3 \text{ s}^{-1}$ ), shutting down the monthly-long, (almost) exponential decay.

338

#### 339 **4.4. Reactivation of Bezymianny in 2016**

340 Strong evidence for volcano-volcano interactions is the lack of the typical extrusive-explosive-effusive cycles  
341 of Bezymianny for four years after the eruption of Tolbachik<sup>73</sup> (Fig. 7a). This rest period was unusually long  
342 for Bezymianny (1550 days) and started already on 11 September 2012 ( $\sim 3$  months before Tolbachik). As  
343 discussed above, the September 2012 eruption of Bezymianny represents the superficial response of its  
344 plumbing system to the main deep magma pulse revealed by DVLP, which heralded a few months later the  
345 eruption of Tolbachik. The following lack of activity at Bezymianny persisted for four years during which  
346 continuous thermal anomalies were likely related to passive degassing (Fig. 7). In early 2016, a viscous,  
347 crystallized, cold plug started to be extruded from the summit crater<sup>74</sup>. This slow, cold extrusion was  
348 undetected by MODIS but, according to Mania et al.<sup>74</sup>, accelerated in September-November 2016 (right at  
349 the end of Klyuchevskoy eruption #9) until the effusion of a viscous lava flow on 9 December 2016 (eruption  
350 #23; Fig. 7). The extrusion of solid plugs at the onset of eruptive cycles is a typical feature of Bezymianny<sup>38,42</sup>.  
351 However, that of 2016 represented an abnormally long precursory phase for this volcano. It was followed by  
352 eruptions #24 and #25, both characterized by a gentle effusion of two lava flows with increasingly stronger  
353 explosivity<sup>74</sup>. This peculiar dynamic after four years of rest seems to be consistent with an interruption (or  
354 decrease) of the magma supply after the TFE that favored the formation of a cold crystallized plug in the  
355 shallow conduit of Bezymianny.





357 **Figure 7** – (a) Stacked TADR time-series for Klyuchevskoy, Bezymianny, and Tolbachik volcanoes between  
 358 2011 and 2018. Eruptive periods for each volcano are labeled according to Table 1. Gray fields outline periods  
 359 of Bezymianny activity characterized by frequent explosive eruptions (stars); (b) The reactivation of  
 360 Bezymianny started in early 2016, through the extrusion of “cold” crystallized plug, undetected by MODIS.  
 361 This anomalous precursory phase culminated in December 2016 (#BEZ23) with the effusion of a new lava  
 362 flow that marks the resumption of activity of Bezymianny after the Tolbachik eruption. Time series generated  
 363 using MATLAB software ([www.mathworks.com](http://www.mathworks.com)).

364  
 365

366  
 367

#### 368 **4.5 Influence of the 1955-56 eruption of Bezymianny and the 1975 Great Tolbachik Fissure Eruption in the** 369 **long term eruptive pattern of Klyuchevskoy and Bezymianny**

370 Bezymianny eruption in 1955-56 (BEZ55) was the largest in the recent history on this volcano<sup>40</sup> and its  
 371 occurrence may have perturbed the whole KVG in some way. Some evidence appears from the analysis of  
 372 the long term volumetric output of Klyuchevskoy (Fig. 1b) which shows an evident reduction in the eruption'  
 373 frequency after 1956, passing from 0.28 events/year, between 1930 and 1953, to 0.17 events/year between  
 374 1956 and 1973 (Fig. 1b). Even more indicative is the fact that this decrease was also associated with an  
 375 evident geochemical change in the products erupted by Klyuchevskoy after 1960<sup>39</sup> (a few years after the  
 376 unrest of Bezymianny), which has been ascribed to the injection of new type of primary magma that was not  
 377 produced beneath the volcano previously.

378 In 1977, immediately after the GTFE, the eruptive regime of Bezymianny changed considerably to give rise,  
 379 for the first time, to the effusion of lava flows and the establishment of extrusive-explosive-effusive  
 380 cycles<sup>43,44</sup>. Simultaneously, the volumetric output rate decelerated (Fig. 1c). The erupted magma became  
 381 more and more primitive, indicating the arrival of deeper mafic magma components at the surface<sup>53</sup>. For

382 Klyuchevskoy, the available data and observations point to a significant change in its eruptive regime starting  
383 1-3 years after the GTFE, when summit eruptions began to dominate over flank eruptions<sup>37</sup> (Fig. 1b). In  
384 contrast to Bezymianny, a significant increase of the output rate accompanied this change likely associated  
385 with an increased magma supply at shallower levels. Geodetic measurements<sup>37</sup> carried out between 1979  
386 and 2005 also suggest that the magma feeding system of Klyuchevskoy was accumulating considerable  
387 amounts of magma before the eruptions of this period, which is coherent with a gradual rise of the effective  
388 pressure source, from the probable region of deep magma storage (25 km) to shallow levels (5 km). Also the  
389 seismicity of the entire KVG showed a dramatic change after the GTFE eruption<sup>22,72</sup> with several remarkable  
390 earthquake swarms that occurred during 1977-1978. All these pieces of evidence make it plausible that both  
391 the BEZ25 and GTFE have perturbed the activity of the neighboring volcanoes, compatibly with a process of  
392 general rejuvenation of the whole KVG magma system. Whether a similar rejuvenation process occurred  
393 during the 2012 Tolbachik eruption is still unclear. However, the occurrence of the major swarms of deep  
394 very-long period events (DVLP) in 2011 and 2012 (Fig. 6) point toward a process of pre-eruptive reload of the  
395 shallow magmatic reservoirs from depth<sup>23</sup>.

396

## 397 5. Discussion

398 Our new satellite data suggest that the three volcanoes of the KVG are related to each other on various time-  
399 scales. The mode and directivity of the relation vary, showing correlated and anti-correlated activity changes.  
400 This observation probably reflects a complex response to changes occurring in a seismically inferred common  
401 magmatic source and/or at the associated hydrothermal system.

402 Conjecturing the presence of crustal magma chambers at the volcano systems, we may develop a  
403 simple conceptual model to explain some of the modulations and concurrent activity changes observed in  
404 our data. At Klyuchevskoy, the magma supply within the crustal plumbing system follows a general steady-  
405 state load and discharge model. The frequent but intermittent arrival of magma batches is buffered by the  
406 elastic deformation of the subvolcanic reservoir<sup>61</sup>. Eruptions occur when the stored amount of magma  
407 exceeds a specific threshold (time-predictable behaviour<sup>65</sup>) with the maximum eruptible volume ( $\sim 150 \times 10^6$   
408  $\text{m}^3$  for Klyuchevskoy; Fig. 3a2) strictly connected to the capacity of the reservoir to buffer the arrival of  
409 magma<sup>53</sup>. It is interesting to note that during the steady-state regime, the magma ascent feeding the activity  
410 at these volcanoes could be driven by processes occurring at depth<sup>61</sup> (down-top mechanism), but also by the  
411 passive degassing during quiescence<sup>62-64</sup>, which induces the opening of pathways connecting deep and  
412 shallow magma reservoir (top-down-mechanism).

413 The eruptive behavior of Bezymianny is also compatible with a steady-state magma supply. However, in this  
414 case, the smaller capacity of the reservoir(s) and the lower magma supply rate (compared to Klyuchevskoy)  
415 give rise to much more frequent but less voluminous eruptions (maximum eruptible volume  $\sim 7 \times 10^6 \text{ m}^3$ ; Fig.

416 3b2). In this steady-state framework, the volcanoes' conjoint activation indicates that both systems  
417 responded to a common perturbation, possibly sourced at lower crustal levels.

418 On the other hand, significant large swarms of DVLP (Fig. 6), ascribed to deep magma pulses, can reactivate  
419 the Tolbachik magmatic path<sup>22,70-72</sup>, which in turn modify the properties of the of nearby magmatic systems  
420 and perturb their steady-state regime.

421 Deviation from the steady-state cumulative volume curve indicates a change in the magma supply rate<sup>61</sup>, as  
422 occurred after the BEZ55 and the GTFE at both Klyuchevskoy and Bezymianny.

423 The GTFE eruption directly affected Bezymianny's activity, causing a reduction of the magma output rate  
424 since 1977 (Fig. 1b2) and producing a radical change in Bezymianny's eruptive regime and a rejuvenation of  
425 its eruptive products<sup>53</sup>. Similarly, but in the opposite direction, the GTFE led to an increase of the long-term  
426 magma output rate of Klyuchevskoy and promoted a change in its eruptive pattern, switching from lateral to  
427 summit eruptions (Fig. 1b1).

428 To a lesser extent, the reactivation of the Tolbachik in 2012 inhibited the steady-state magma supply of  
429 Bezymianny for several years. It caused the interruption of its surface activity until the extrusion of a  
430 crystallized plug in 2016 (Fig.7). During this period, multiple interactions between Tolbachik and  
431 Klyuchevskoy were also observed, supporting the existence of a very efficient hydraulic connection between  
432 the plumbing systems of the three volcanoes. We note that the details on the presence of a common primary  
433 magma feeding all volcanoes in KVG as well as the location and geometry of crustal magma chambers are  
434 still debated<sup>19,36</sup>, which is why our conceptual model remains speculative.

435 Shapiro et al.<sup>22</sup> proposed a model based on fluid-pressure propagation through porous rocks to explain the  
436 migration of LP events and infer the existence of such hydraulic connections below the KVG volcanoes. Our  
437 data supports and reinforces this hypothesis, although other processes can also influence the eruption cycles  
438 and dynamics<sup>75</sup>. Independent of any model assumption, our data show that the magmatic systems below the  
439 KVG are interconnected, and eruptions of individual volcanoes can be the direct consequence of their  
440 neighbors' activity.

441 To what extend magmatic systems are connected and if one eruption can trigger another volcano are  
442 essential questions for assessing volcanic hazard. In the case of interacting volcanoes, such as in the case of  
443 KVG, a volcano's behavior can be the direct consequence of its neighbor's activity. In these cases, traditional  
444 hazard assessments of isolated volcanoes have to be replaced by a comprehensive assessment involving the  
445 whole volcanic group. In addition to its eruptive history, the volcano's hazard assessment has to account for  
446 its neighboring volcanoes' eruptive history, which may influence its current state.

447

448

## 449 **Methods**

### 450 ***Satellite Thermal data***

451 Satellite thermal data were processed using the MIROVA system<sup>60</sup> ([www.mirovaweb.it](http://www.mirovaweb.it)), which is based on  
452 the analysis of the images acquired by MODIS. The two MODIS sensors, launched in March 2000 and May  
453 2002, provide approximately six infrared images per day over Kamchatka (three night-times and three day-  
454 times) with a nominal ground resolution of 1 km. MODIS images are processed at each volcano to quantify  
455 the Volcanic Radiative Power (VRP in Watts), a combined measurement of the area and integrated  
456 temperature of the hot (>200°C) volcanic features with a standard error of  $\pm 30\%$  over every  
457 measurement<sup>60</sup>.

458 We used only the night-time MODIS dataset, consisting of approximately 19,500 images acquired over the  
459 Klyuchevskoy Volcanic Group (KVG). Thermal anomalies detected by MIROVA were geolocated (errors in  
460 geolocation are less than 0.5 km for nadir acquisition<sup>60</sup>) to discriminate the hotspots sourced by the three  
461 distinct volcanoes. All the images were visually analyzed to discard the data contaminated by clouds, ash  
462 plumes, or poor viewing conditions (i.e., high satellite zenith), which preclude a correct estimation of VRP<sup>15,52</sup>.  
463 Finally, the supervised dataset consists of 2,139 images for Klyuchevskoy, 2013 images for Bezymianny, and  
464 219 images for Tolbachik, which have been used to reconstruct the time-series of VRP (*Fig. S1 -*  
465 *Supplementary Material*). For each volcano, the cumulative Volcanic Radiative Energy (VRE) in Joules is  
466 calculated as the trapezoidal integration of the supervised VRP time series (*Fig. S1 - Supplementary Material*).

#### 467 ***Erupted volume and Time-Averaged lava Discharge Rate***

468 We used a simplified approach, which has been expressly developed to derive Time Averaged lava discharge  
469 Rate (TADR) directly from MODIS-derived VRP<sup>76</sup>. This approach assumes that during an eruption, the energy  
470 radiated by a lava body (i.e., VRE) is linearly correlated to the bulk erupted volume (Vol),

$$471 \quad c_{rad} = \frac{VRE}{Vol} \quad (\text{eq. 1}),$$

472 where  $c_{rad}$  (in  $\text{J m}^{-3}$ ) is the best-fit coefficient that describes the ability to radiate thermal energy by unit  
473 volume of the observed lava body. Thus the  $c_{rad}$  value can be determined retrospectively by measuring the  
474 energy radiated during an eruption (or during an eruptive period) and the bulk volume of the lava flow(s) or  
475 domes emplaced during the same time interval (measured independently).

476 Once calibrated, the  $c_{rad}$  coefficient is used to retrieve the TADR for each single VRP measurements according  
477 to

$$478 \quad TADR = \frac{VRP}{c_{rad}} \quad (\text{eq. 2}).$$

479 Note that this approach does not take into account the volume of magma erupted explosively (i.e., ash  
480 plumes, pyroclastic density currents). It accounts only for magma erupted during effusive/extrusive periods,  
481 that is, when sufficient thermal radiation is detectable from the satellite.

482 To estimate the  $c_{\text{rad}}$ -value of Klyuchevskoy, we considered the period between 2002 and 2009, during which  
 483 about  $231 \times 10^6 \text{ m}^3$  of lava erupted<sup>21</sup>. Assuming an average fraction of tephra equal to 15% in volume<sup>37</sup>, the  
 484 cumulative volume of lava flows erupted between 2002 and 2009 become  $\sim 196 \times 10^6 \text{ m}^3$ . This activity  
 485 produced a VRE of  $1.6 \times 10^{16} \text{ J}$  (Fig. S1c1 - Supplementary Material), which results into an average  $c_{\text{rad}}$ -value  
 486 of  **$8.16 \times 10^7 \text{ J m}^{-3}$** .

487 For Bezymianny volcano, we calibrated the  $c_{\text{rad}}$ , by considering the dome volume's growth between 31 July  
 488 2006 and 9 September 2017<sup>44</sup>. Given a total volume of  $\sim 69 \times 10^6 \text{ m}^3$  and a VRE of  $1.17 \times 10^{15} \text{ J}$  (Fig. S1c2 -  
 489 Supplementary Material), we estimated  $c_{\text{rad}} = \mathbf{1.88 \times 10^7 \text{ J m}^{-3}}$ . Note that the TADR and inferred volumes do  
 490 not include the contribution of the explosive activity, which in the case of Bezymianny may be relevant.  
 491 According to Girina et al.<sup>42</sup>, each extrusive-explosive-effusive cycle produces volumes up to  $\sim 10^7 \text{ m}^3$ , in the  
 492 form of pyroclastic flows. Although the amount of juvenile material inside these deposits is unknown, the  
 493 large amount of material erupted explosively, together with the short duration of each cycle, introduces a  
 494 significant level of noise into our time series and an uncertainty possibly higher than 100% in the volumes  
 495 reported in Table 1b.

496 Equations 1 and 2 have been successfully applied to estimate the TADRs of the 2012-2013 Tolbachik  
 497 eruption<sup>67</sup>, where a  $c_{\text{rad}}$  equal to  **$1.08 \times 10^8 \text{ J m}^{-3}$**  has been calculated based on a final lava flow volume<sup>77</sup> of  
 498  $573 \times 10^6 \text{ m}^3$  and a corresponding VRE equal to  $6.07 \times 10^{16}$  (Fig. S1c2 - Supplementary Material).

499 As described by Coppola et al.<sup>76</sup>, this approach provides single TADR measurements with an associated error  
 500 of  $\pm 50\%$ . Errorbars are not shown for graphical convenience.

501

### 502 **Statistical testing of correlated activity**

503 The frequency plot of inter-eruption time ( $dt_{\text{es}}$  in Tab 1) for Bezymianny and Klyuchevskoy is shown in the  
 504 left axis of Fig. 4. The peaked distribution for Bezymianny data (gray bars in Fig. 4a,b) can be reasonably fitted  
 505 by a Brownian-Passage Time (BPT) distribution (blue line). This models assumes a fixed eruption threshold  
 506 and volume release, plus a constant loading rate with noise. The coefficient of variation (CV), also called the  
 507 aperiodicity parameter, measures a signal's periodicity, where  $CV=0$  refers to a perfect periodicity,  $CV=1$  to  
 508 a random Poisson occurrence, and  $CV>1$  to clustering. When considering the whole dataset of Bezymianny  
 509 (Fig. 4a), the CV value is 1.20, indicating a random occurrence of eruptions. However, the CV value decreases  
 510 to 0.50 when post-Tolbachik eruption data are excluded (Fig. 4b), thus indicating a quasi-periodic behavior  
 511 until the Tolbachik eruption. For Klyuchevskoy (Fig. 4c), the CV value is even lower ( $CV=0.38$ ), indicating a  
 512 rather clock-wise recurrence of eruptions.

513 The relation between inter-eruption time and volume release of the last or next event is shown on the right  
 514 axis of Fig. 4. The data shows no correlations for Bezymianny ( $p$ -values  $> 0.25$  in Fig. 4a,b), while  $p<0.05$  would  
 515 indicate a statistically significant correlation. In contrast, Klyuchevskoy (Fig. 4c) shows a positive correlation

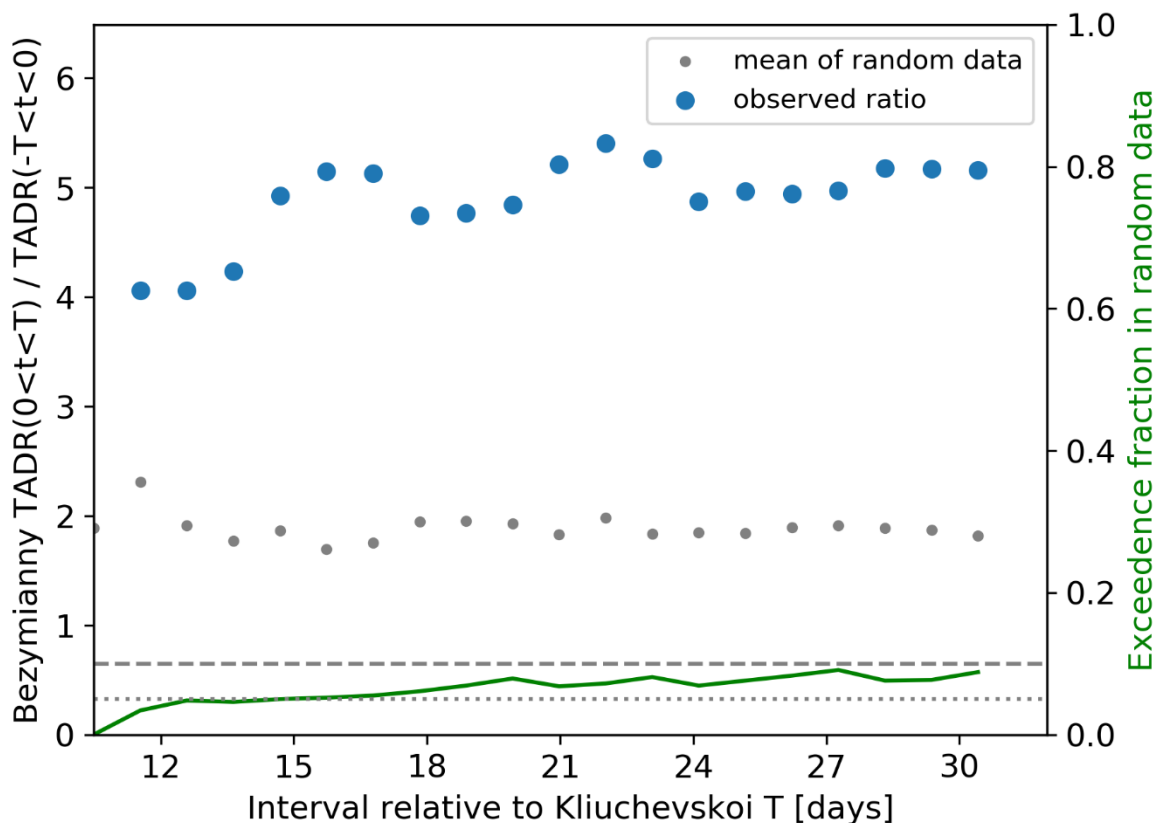
516 between the inter-eruption time and the volume of the last eruption ( $r=0.65$ ,  $p=0.081$ ), which become  
517 statistically significant ( $r=0.73$ ;  $p=0.025$ ) when including the timing of the last eruption (not included in our  
518 study) started in November 2019<sup>66</sup>. The weaker correlation with the next events' volume found for the  
519 Kluchevskoi volcano (Fig. 4c) suggests that its eruption periodicity is consistent with a time-predictable rather  
520 than a volume-predictable model.

521

### 522 **Conjoint activity of Klyuchevskoy and Bezymianny volcanoes**

523 We tested the hypothesis that before the Tolbachik eruption, the activation of Klyuchevskoy (eruptions #1  
524 to 6) affected the Bezymianny activity (Fig. S4). To perform this test, we first calculated the average TADR-  
525 value (of Bezymianny) within T days (from 10 to 30 days) relative to each Klyuchevskoy eruption and averaged  
526 those six values. Then we calculated the ratio between the averaged TADR-value in the T days after the  
527 eruption and the corresponding value in the T days before the eruption to measure the average activation  
528 (blue points in figure 8). Finally, we compared the observed ratio (as a function of T) with the corresponding  
529 result obtained after randomizing the activation times of the six Klyuchevskoy eruptions within the period  
530 between 2002 and the Tolbachik eruption. The fraction of randomized data with a ratio similar or larger than  
531 the observed one (green line in Fig. 8) shows that the observed activation value can only be reached in less  
532 than 5-10% of the randomized data. Although the results are close to the significance threshold, these data  
533 suggest that the result is significant for the shortest time intervals (i.e.,  $T=10$  days;  $p<0.05$ ) with a 4-5 times  
534 increase of the averaged TADR of Bezymianny after the onset of a Klyuchevskoy eruption.

535 Note that we have not analyzed  $T<10$  days because of missing Bezymianny measurements during short  
536 periods before/after the Klyuchevskoy eruptions.



537

538 **Figure 8** – (Left Axis) Ratio between the averaged Bezymianny TADR values within T days after and before  
 539 the Klyuchevskoy eruptions (#1 to 6). (Right axis). Mean fraction in randomized data that exceeded the observed  
 540 ratio (see the text for more explanations).

541

542 **Data Availability**

543 The satellite datasets are available as Supplementary Material at:

544

545 **Tables**

546 **Table 1a** – Eruptions and parameters of Klyuchevskoy volcano retrieved from MODIS data. Volumes, TADR  
 547 and MOR are calculated as bulk values (see *Methods*)

548

erupti on	start	peak	end	durati on	dt_es	Vol	TADRma x	MOR
#	dd/mm/yyyy hh:mm	dd/mm/yyyy hh:mm	dd/mm/yyyy hh:mm	days	days	$\times 10^6 m^3$	$m^3 s^{-1}$	$m^3 s^{-1}$
1	23/07/2003 16:10	07/11/2003 10:10	24/01/2004 16:05	186.90	N.d.	7.3	2.7	0.5
2	14/01/2005 15:40	07/02/2005 16:25	28/03/2005 11:30	73.60	356.0	52.3	40.7	8.2
3	18/03/2007 15:35	22/05/2007 10:35	18/06/2007 10:15	103.50	720.2	85.4	58.2	9.5

4	15/10/2008 16:20	30/11/2008 10:50	07/01/2009 15:55	86.20	485.3	45.2	38.2	6.1
5	20/09/2009 10:10	28/08/2010 11:10	28/10/2010 16:25	441.60	255.8	151.5	54.1	4.0
6*	09/09/2012 15:35	04/11/2012 10:40	07/01/2013 10:40	119.80	681.97	0.15	0.1	0.01
7	13/08/2013 15:10	16/10/2013 11:05	25/10/2013 11:00	75.10	218.2	94.6	93.9	14.6
8	01/01/2015 10:05	14/01/2015 15:15	23/02/2015 10:25	55.80	433.0	12.3	10.2	2.6
9	06/04/2016 15:20	05/09/2016 14:25	01/11/2016 16:00	211.80	408.2	137.8	24.8	7.5
10**	11/11/2019	n.d.	n.d.	n.d.	1104.3 33	n.d.	n.d.	n.d.

549

550

551

552

553

554

555

\* Eruption #6 was detected by MODIS but with TADR  $< 0.25 \text{ m}^3 \text{ s}^{-1}$ . Eruption start and end, are selected manually based on first and last thermal anomalies.

\*\* Start of Eruption#10 from<sup>36</sup>

**Table 1b – Continue.** Eruptions and parameters of Bezymianny retrieved from MODIS data.

Volumes, TADR and MOR are calculated as bulk values (see Methods)

event #	Date Exp.*	start	peak	end	duration days	dt_p days	dt_e days	Vol $\times 10^6$ $\text{m}^3$	TADR max $\text{m}^3 \text{ s}^{-1}$	MOR $\text{m}^3 \text{ s}^{-1}$
1	13/03/ 2000	04/03/200 0 05:30	18/03/200 0 11:35	24/04/200 0 08:01	51.1	nan	nan	3.5	4.2	0.8
2	01/11/ 2000	27/09/200 0 15:42	01/11/200 0 11:05	16/11/200 0 18:10	50.1	228. 0	156. 3	14.2	51.9	3.3
3	06/08/ 2001	22/07/200 1 09:52	06/08/200 1 10:25	23/08/200 1 21:20	32.5	278. 0	247. 7	10.9	30.9	3.9
4	16/12/ 2001	28/11/200 1 17:20	13/12/200 1 11:05	01/01/200 2 23:58	34.3	129. 0	96.8	8.1	20.7	2.7
5	25/12/ 2002	12/12/200 2 20:43	25/12/200 2 14:55	07/01/200 3 20:17	26.0	377. 2	344. 9	4.8	50.9	2.1
6	26/07/ 2003	13/07/200 3 00:25	26/07/200 3 15:15	10/08/200 3 16:45	28.7	213. 0	186. 2	5.3	16.1	2.1
7	13/01/ 2004	06/01/200 4 17:04	14/01/200 4 10:00	23/01/200 4 22:43	17.2	171. 8	149. 0	0.6	3.2	0.4
8	18/06/ 2004	03/06/200 4 22:01	19/06/200 4 15:10	30/06/200 4 13:43	26.7	157. 2	132. 0	1.6	2.0	0.7
9	11/01/ 2005	10/01/200 5 13:02	16/01/200 5 15:40	20/01/200 5 22:28	10.4	211. 0	194. 0	0.3	0.4	0.3
10	30/11/ 2005	16/11/200 5 15:08	30/11/200 5 11:50	16/12/200 5 00:15	29.4	317. 8	299. 7	6.4	12.8	2.5
11	09/05/ 2006	29/04/200 6 07:39	08/05/200 6 11:05	27/05/200 6 23:59	28.7	159. 0	134. 3	1.1	0.9	0.5
12	24/12/ 2006	15/12/200 6 18:15	23/12/200 6 11:25	03/01/200 7 10:45	18.7	229. 0	201. 8	0.8	1.5	0.5
13	11/05/ 2007	29/04/200 7 13:39	12/05/200 7 15:55	07/06/200 7 08:13	38.8	140. 2	116. 1	6.1	18.5	1.8



14	14/10/ 2007	16/09/200 7 08:57	15/10/200 7 14:40	05/11/200 7 22:31	50.6	155. 9	101. 0	2.3	1.7	0.5
15*	05/11/ 2007	N.d.	05/11/200 7	N.d.	N.d.	N.d.	N.d.	N.d.	N.d.	N.d.
16	19/08/ 2008	02/08/200 8 08:08	11/08/200 8 11:45	06/09/200 8 17:04	35.4	300. 9	270. 4	1.8	3.7	0.6
17	16/12/ 2009	03/12/200 9 00:28	17/12/200 9 15:20	07/01/201 0 16:41	35.7	493. 1	452. 3	5.8	8.2	1.9
18	16/02/ 2010	26/01/201 0 18:46	09/02/201 0 14:40	27/02/201 0 01:27	31.3	54.0	19.1	2.3	2.7	0.9
19	31/05/ 2010	10/05/201 0 19:28	29/05/201 0 15:50	15/06/201 0 23:40	36.2	109. 0	72.8	2.6	2.5	0.8
20	13/04/ 2011	31/03/201 1 14:07	15/04/201 1 10:50	02/05/201 1 23:11	32.4	320. 8	288. 6	2.3	4.1	0.8
21	08/03/ 2012	14/02/201 2 06:58	08/03/201 2 15:40	21/03/201 2 13:33	36.3	328. 2	287. 3	7.3	34.2	2.3
22	01/09/ 2012	24/08/201 2 16:26	04/09/201 2 15:15	15/09/201 2 10:18	21.7	180. 0	156. 1	0.8	1.0	0.4
23	15/12/ 2016	03/12/201 6 04:34	12/12/201 6 16:05	28/12/201 6 01:00	24.9	1560 .0	1539 .8	1.9	3.0	0.9
24	09/03/ 2017	11/02/201 7 10:06	09/03/201 7 16:10	30/03/201 7 06:56	46.9	87.0	45.4	4.1	5.8	1.0
25	16/06/ 2017	09/06/201 7 17:46	26/06/201 7 15:40	12/09/201 7 23:24	95.2	109. 0	71.5	4.8	1.9	0.6
26	20/12/ 2017	21/12/201 7 19:22	22/12/201 7 02:45	07/01/201 8 04:41	16.4	178. 5	99.8	0.4	0.4	0.3
27	20/01/ 2019	24/01/201 9 08:01	26/01/201 9 16:10	30/01/201 9 22:18	6.6	400. 6	382. 1	0.2	2.7	0.3
28	15/03/ 2019	06/03/201 9 19:19	15/03/201 9 10:30	27/03/201 9 18:59	21.0	47.8	34.9	0.9	0.8	0.5
29	N.d.	05/12/201 9 22:01	12/12/201 9 10:30	24/12/201 9 02:32	18.2	272. 0	253. 1	0.6	0.4	0.4

\*Date of explosion from Ozerov et al.<sup>38</sup>

\*\*Event #15 not detected by MODIS but reported in Ozerov et al.<sup>38</sup>

556  
557  
558  
559  
560

## 561 References

- 562 1. Sturkell, E. et al. 2 Katla and Eyjafjallajökull Volcanoes. Developments in Quaternary Sciences The  
563 Mýrdalsjökull Ice Cap, Iceland. Glacial processes, sediments and landforms on an active volcano 5–  
564 21 (2010). doi:10.1016/s1571-0866(09)01302-5
- 565 2. Hildreth, W. & Fierstein, J. Katmai volcanic cluster and the great eruption of 1912. Geological Society  
566 of America Bulletin 112, 1594–1620 (2000).
- 567 3. Eichelberger, J. C. & Izbekov, P. E. Eruption of andesite triggered by dyke injection: contrasting cases  
568 at Karymsky Volcano, Kamchatka and Mt Katmai, Alaska. Philosophical Transactions of the Royal  
569 Society of London. Series A: Mathematical, Physical and Engineering Sciences 358, 1465–1485 (2000).

- 570 4. Gusev, A. A., Ponomareva, V. V., Braitseva, O. A., Melekestsev, I. V. & Sulerzhitsky, L. D. Great  
571 explosive eruptions on Kamchatka during the last 10,000 years: Self-similar irregularity of the  
572 output of volcanic products. *Journal of Geophysical Research: Solid Earth* 108, (2003).
- 573 5. Walter, T. et al. Possible coupling of Campi Flegrei and Vesuvius as revealed by InSAR time series,  
574 correlation analysis and time dependent modeling. *Journal of Volcanology and Geothermal Research*  
575 280, 104–110 (2014).
- 576 6. Miklius, A. & Cervelli, P. Interaction between Kilauea and Mauna Loa. *Nature* 421, 229–229 (2003).
- 577 7. Biggs, J., Robertson, E. & Cashman, K. The lateral extent of volcanic interactions during unrest and  
578 eruption. *Nature Geoscience* 9, 308–311 (2016).
- 579 8. Kutterolf, S. et al. A detection of MILANKOVITCH frequencies in global volcanic activity. *Geology* 41,  
580 227–230 (2013).
- 581 9. Nostro, C., Stein, R. S., Cocco, M., Belardinelli, M. E. & Marzocchi, W. Two-way coupling between  
582 Vesuvius eruptions and southern Apennine earthquakes, Italy, by elastic stress transfer. *Journal of*  
583 *Geophysical Research: Solid Earth* 103, 24487–24504 (1998).
- 584 10. Hill, D. P., Pollitz, F. & Newhall, C. Earthquake–Volcano Interactions. *Physics Today* 55, 41–47 (2002).
- 585 11. Walter, T. R. & Amelung, F. Volcanic eruptions following  $M \geq 9$  megathrust earthquakes: Implications  
586 for
- 587 12. Watt, S. F., Pyle, D. M. & Mather, T. A. The influence of great earthquakes on volcanic eruption rate  
588 along the Chilean subduction zone. *Earth and Planetary Science Letters* 277, 399–407 (2009).
- 589 13. Kennedy, B. What effects do earthquakes have on volcanoes? *Geology* 45, 765–766 (2017).
- 590 14. Seropian, G., Kennedy, B.M., Walter, T.R. et al. A review framework of how earthquakes trigger  
591 volcanic eruptions. *Nat Commun* 12, 1004 (2021).
- 592 15. Dzurisin, D. & Poland, M. P. Magma supply to Kīlauea Volcano, Hawai‘i, from inception to now:  
593 Historical perspective, current state of knowledge, and future challenges. *Field Volcanology: A*  
594 *Tribute to the Distinguished Career of Don Swanson* (2019). doi:10.1130/2018.2538(12)
- 595 16. Gonnermann, H. M. et al. Coupling at Mauna Loa and Kīlauea by stress transfer in an asthenospheric  
596 melt layer. *Nature Geoscience* 5, 826–829 (2012).
- 597 17. Coppola, D. et al. Thermal Remote Sensing for Global Volcano Monitoring: Experiences From the  
598 MIROVA System. *Frontiers in Earth Science* 7, (2020).
- 599 18. Koulakov, I. et al. Three different types of plumbing system beneath the neighbouring active  
600 volcanoes of Tolbachik, Bezymianny, and Klyuchevskoy in Kamchatka. *Journal of Geophysical*  
601 *Research: Solid Earth* 122, 3852–3874 (2017).
- 602 19. Kayzar, T.M., Nelson, B.K., Bachmann, O., Bauer, A.M., Izbekov, P.E.. Deciphering petrogenic  
603 processes using Pb isotope ratios from time-series samples at Bezymianny and Klyuchevskoy  
604 volcanoes, Central Kamchatka Depression. *Contrib Mineral Petrol* 168:1067 (2014).

- 605 20. Cashman K.V., Sparks, R.S., & , J.D. Vertically extensive and unstable magmatic systems: A unified  
606 view of igneous processes. *Science* 355, eaag3055 (2017).
- 607 21. Fedotov, S. A., Zharinov, N. A. & Gontovaya, L. I. The magmatic system of the Klyuchevskaya group of  
608 volcanoes inferred from data on its eruptions, earthquakes, deformation, and deep structure. *Journal*  
609 *of Volcanology and Seismology* 4, 1–33 (2010).
- 610 22. Shapiro, N. M. et al. Deep and shallow long-period volcanic seismicity linked by fluid-pressure  
611 transfer. *Nature Geoscience* 10, 442–445 (2017).
- 612 23. Chebrov, V.N., Voropaev, V.F., Droznin, D.V., Sergeev, V.A., & Shevchenko, Yu.V., Development of  
613 digital seismic network in Kamchatka, in *Geofizicheskii monitoring Kamchatki (Geophysical*  
614 *Monitoring in Kamchatka)*, Chebrov, V.N. and Kopylova, G.N., Eds., Petropavlovsk-Kamchatskii, pp.  
615 13–20 (2006)
- 616 24. Khubunaya, S. A., Gontovaya, L. I., Sobolev, A. V. & Nizkous, I. V. Magma chambers beneath the  
617 Klyuchevskoy volcanic group (Kamchatka). *Journal of Volcanology and Seismology* 1, 98–118 (2007).
- 618 25. Shapiro N.M., C. Sens-Schönfelder, B. Lühr, M. Weber, I. Abkadyrov, E.I. Gordeev, I. Koulakov, A.  
619 Jakovlev, Y. Kugaenko, and V. Saltykov. Understanding Kamchatka’s Extraordinary Volcano Cluster.  
620 EOS, DOI: 10.1029/2017eo071351. (2017)
- 621 26. Koulakov, I., Plechov, P., Mania, R. et al. Anatomy of the Bezymianny volcano merely before an  
622 explosive eruption on 20.12.2017. *Sci Rep* 11, 1758 (2021).
- 623 27. Melekestsev, I. V.. *Volcanism and relief formation (in Russian)*. Moscow: Nauka (1980).
- 624 28. Churikova, T., Dorendorf, F. & Wörner, G. Sources and Fluids in the Mantle Wedge below Kamchatka,  
625 Evidence from Across-arc Geochemical Variation. *Journal of Petrology* 42, 1567–1593 (2001).
- 626 29. Münker, C., Wörner, G., Yogodzinski, G. & Churikova, T. Behaviour of high field strength elements in  
627 subduction zones: constraints from Kamchatka–Aleutian arc lavas. *Earth and Planetary Science*  
628 *Letters* 224, 275–293 (2004).
- 629 30. Green, R. G., Sens-Schönfelder, C., Shapiro, N., Koulakov, I., Tilmann, F., Dreiling, J., et al. Magmatic  
630 and sedimentary structure beneath the Klyuchevskoy Volcanic Group, Kamchatka, from ambient  
631 noise tomography. *Journal of Geophysical Research: Solid Earth* 125, e2019JB018900 (2020).
- 632 31. Koulakov, I., Shapiro, N. M., Sens-Schönfelder, C., Luehr, B. G., Gordeev, E. I., Jakovlev, A., et al..  
633 Mantle and crustal sources of magmatic activity of Klyuchevskoy and surrounding volcanoes in  
634 Kamchatka inferred from earthquake tomography. *Journal of Geophysical Research: Solid Earth* 125,  
635 e2020JB020097 (2020).
- 636 32. Levin, V., Shapiro, N. M., Park, J., & Ritzwoller, M. H.. Slab portal beneath the western Aleutians.  
637 *Geology* 33(4), 253–256 (2005).
- 638 33. Levin V., Shapiro N. M., Park, J., & Ritzwoller M.H.. Seismic evidence for catastrophic slab loss  
639 beneath Kamchatka. *Nature* 418, 763-767 (2002).

- 640 34. Dorendorf, F., Wiechert, U. & Wörner, G. Hydrated sub-arc mantle: a source for the Kluchevskoy  
641 volcano, Kamchatka/Russia. *Earth and Planetary Science Letters* 175, 69–86 (2000).
- 642 35. Portnyagin, M., Bindeman, I., Hoernle, K. & Hauff, F. Geochemistry of primitive lavas of the Central  
643 Kamchatka Depression: Magma generation at the edge of the Pacific Plate. *Volcanism and*  
644 *Subduction: The Kamchatka Region* 199–239 (2007). doi:10.1029/172gm16
- 645 36. Ozerov, A.Y., Ariskin, A.A., Kyle, P., Bogoyavlenskaya, G.E., Karpenko, S.F. Petrological–geochemical  
646 model for genetic relationships between basaltic and andesitic magmatism of Klyuchevskoi and  
647 Bezymyanni volcanoes, Kamchatka. *Petrology* 5, 550–569 (1997)
- 648 37. Fedotov, S. A. & Zharinov, N. A. On the eruptions, deformation, and seismicity of Klyuchevskoy  
649 Volcano, Kamchatka in 1986–2005 and the mechanisms of its activity. *Journal of Volcanology and*  
650 *Seismology* 1, 71–97 (2007).
- 651 38. Ozerov, A. Y., Girina, O. A., Zharinov, N. A., Belousov, A. B. & Demyanchuk, Y. V. Eruptions in the  
652 Northern Group of Volcanoes, in Kamchatka, during the Early 21st Century. *Journal of Volcanology*  
653 *and Seismology* 14, 1–17 (2020).
- 654 39. Bergal-Kuvikas, O. et al. A petrological and geochemical study on time-series samples from  
655 Klyuchevskoy volcano, Kamchatka arc. *Contributions to Mineralogy and Petrology* 172, (2017).
- 656 40. Gorshkov, G.S. Gigantic eruption of the volcano Bezymianny. *Bull Volcanol* 20, 77–109 (1959).  
657 <https://doi.org/10.1007/BF02596572>
- 658 41. Zharinov, N. A. & Demyanchuk, Y. V. Assessing the Volumes of Material Discharged by Bezymyanni  
659 Volcano during the 1955–2009 Period. *Journal of Volcanology and Seismology* 5(2), 100–113 (2011).
- 660 42. Girina, O. A. Chronology of Bezymianny Volcano activity, 1956–2010. *Journal of Volcanology and*  
661 *Geothermal Research* 263, 22–41 (2013).
- 662 43. Bogoyavlenskaya, G. E., Ivanov, B.V., Budnikov, V.A., Andreev, V.N. Eruption of Bezymianny volcano  
663 in 1977. *Bull. Volcanol. Stat.* 57, 16–25 (1979) (In Russian).
- 664 44. Shevchenko, A. V. et al. The rebirth and evolution of Bezymianny volcano, Kamchatka after the 1956  
665 sector collapse. *Communications Earth & Environment* 1, (2020).
- 666 45. Carter, A. J., Ramsey, M. S. & Belousov, A. B. Detection of a new summit crater on Bezymianny  
667 Volcano lava dome: satellite and field-based thermal data. *Bulletin of Volcanology* 69, 811–815  
668 (2007).
- 669 46. Manen, S. M. V., Dehn, J. & Blake, S. Satellite thermal observations of the Bezymianny lava dome  
670 1993–2008: Precursory activity, large explosions, and dome growth. *Journal of Geophysical Research*  
671 115, (2010).
- 672 47. Manen, S. M. V., Blake, S., Dehn, J. & Valcic, L. Forecasting large explosions at Bezymianny Volcano  
673 using thermal satellite data. *Geological Society, London, Special Publications* 380, 187–201 (2013).

- 674 48. Girina, O. A. On precursor of Kamchatkan volcanoes eruptions based on data from satellite  
675 monitoring. *Journal of Volcanology and Seismology* 6, 142–149 (2012).
- 676 49. Reath, K., Ramsey, M., Dehn, J. & Webley, P. Predicting eruptions from precursory activity using  
677 remote sensing data hybridization. *Journal of Volcanology and Geothermal Research* 321, 18–30  
678 (2016).
- 679 50. Ivanov, A. et al. Magma source beneath the Bezymianny volcano and its interconnection with  
680 Klyuchevskoy inferred from local earthquake seismic tomography. *Journal of Volcanology and*  
681 *Geothermal Research* 323, 62–71 (2016).
- 682 51. Davydova, V. O., Shcherbakov, V. D., Plechov, P. Y. & Perepelov, A. B. Petrology of mafic enclaves in  
683 the 2006–2012 eruptive products of Bezymianny Volcano, Kamchatka. *Petrology* 25, 592–614 (2017).
- 684 52. Shcherbakov, V. D., Plechov, P. Y., Izbekov, P. E. & Shipman, J. S. Plagioclase zoning as an indicator of  
685 magma processes at Bezymianny Volcano, Kamchatka. *Contributions to Mineralogy and Petrology*  
686 162, 83–99 (2010).
- 687 53. Turner, S. J., Izbekov, P. & Langmuir, C. The magma plumbing system of Bezymianny Volcano: Insights  
688 from a 54year time series of trace element whole-rock geochemistry and amphibole compositions.  
689 *Journal of Volcanology and Geothermal Research* 263, 108–121 (2013).
- 690 54. Thelen, W., West, M. & Senyukov, S. Seismic characterization of the fall 2007 eruptive sequence at  
691 Bezymianny Volcano, Russia. *Journal of Volcanology and Geothermal Research* 194, 201–213 (2010).
- 692 55. Churikova, T., Gordeychik, B., Edwards, B., Ponomareva, V. & Zelenin, E. The Tolbachik volcanic  
693 massif: A review of the petrology, volcanology and eruption history prior to the 2012–2013 eruption.  
694 *Journal of Volcanology and Geothermal Research* 307, 3–21 (2015).
- 695 56. Fedotov, S. A., Chirkov, A. M., Gusev, N. A., Kovalev, G. N. & Slezin, Y. B. The large fissure eruption in  
696 the region of Plosky Tolbachik volcano in Kamchatka, 1975–1976. *Bulletin Volcanologique* 43, 47–60  
697 (1980).
- 698 57. Belousov, A., Belousova, M., Edwards, B., Volynets, A. & Melnikov, D. Overview of the precursors and  
699 dynamics of the 2012–13 basaltic fissure eruption of Tolbachik Volcano, Kamchatka, Russia. *Journal*  
700 *of Volcanology and Geothermal Research* 299, 19–20 (2015).
- 701 58. Dvigalo, V. N., Svirid, I. Y. & Shevchenko, A. V. The first quantitative estimates of parameters for the  
702 Tolbachik Fissure Eruption of 2012–2013 from aerophotogrammetric observations. *Journal of*  
703 *Volcanology and Seismology* 8, 261–268 (2013).
- 704 59. Lundgren, P., Kiryukhin, A., Milillo, P., Samsonov, S. Dike model for the 2012–2013 Tolbachik eruption  
705 constrained by satellite radar interferometry observations. *Journal of Volcanology and Geothermal*  
706 *Research*, 307, 79–88 (2015)

- 707 60. Coppola, D., Laiolo, M., Cigolini, C., Donne, D. D. & Ripepe, M. Enhanced volcanic hot-spot detection  
708 using MODIS IR data: results from the MIROVA system. *Geological Society, London, Special*  
709 *Publications* 426, 181–205 (2015).
- 710 61. Wadge, G. Steady state volcanism: Evidence from eruption histories of polygenetic volcanoes. *Journal*  
711 *of Geophysical Research* 87, 4035 (1982).
- 712 62. Girona, T., Costa, F., Newhall, C., Taisne, B. On depressurization of volcanic magma reservoirs by  
713 passive degassing. *Journal of Geophysical Research: Solid Earth* 119 (12), 8667-8687 (2014)
- 714 63. Girona, T., Costa, F., Schubert, G. Degassing during quiescence as a trigger of magma ascent and  
715 volcanic eruptions. *Scientific reports* 5 (1), 1-7 (2015)
- 716 64. Mittal, T., Richards, MA. Volatile degassing from magma chambers as a control on volcanic  
717 eruptions. *Journal of Geophysical Research: Solid Earth* 124 (8), 7869-7901 (2019)
- 718 65. Cruz-Reyna, S. D. L. Poisson-distributed patterns of explosive eruptive activity. *Bulletin of Volcanology*  
719 54, 57–67 (1991).
- 720 66. Global Volcanism Program. Report on Klyuchevskoy (Russia) (Krippner, J.B., and Venzke, E., eds.).  
721 *Bulletin of the Global Volcanism Network*, 45:6. Smithsonian Institution (2020)
- 722 67. Ramsey, M.S., Chevrel, M.O., Coppola, D. & Harris, A.J.L.. The influence of emissivity on the thermos-  
723 rheological modeling of the channelized lava flows at Tolbachik volcano. *Annals of Geophysics* 62(2),  
724 V0222 (2019).
- 725 68. Laiolo, M., Ripepe, M., Cigolini, C., Coppola, D., Della Schiava, M., Genco, R., Innocenti, L., Lacanna,  
726 G., Marchetti, E., Massimetti, F., Silengo, M.C. Space- and Ground-Based Geophysical Data Tracking  
727 of Magma Migration in Shallow Feeding System of Mount Etna Volcano. *Remote Sens.* 11(10), 1182  
728 (2019).
- 729 69. Reath, K. et al. Thermal, Deformation, and Degassing Remote Sensing Time Series (CE 2000–2017) at  
730 the 47 most Active Volcanoes in Latin America: Implications for Volcanic Systems. *Journal of*  
731 *Geophysical Research: Solid Earth* 124, 195–218 (2019).
- 732 70. Frank, W. B., Shapiro, N. M. & Gusev, A. A. Progressive reactivation of the volcanic plumbing system  
733 beneath Tolbachik volcano (Kamchatka, Russia) revealed by long-period seismicity. *Earth and*  
734 *Planetary Science Letters* 493, 47–56 (2018).
- 735 71. Melnik, O., Lyakhovsky, V., Shapiro, N. M., Galina, N. & Bergal-Kuvikas, O. Deep long period volcanic  
736 earthquakes generated by degassing of volatile-rich basaltic magmas. *Nature Communications* 11,  
737 (2020).
- 738 72. Fedotov, S.A., Slavina, L. B., Senyukov, S. L., Kuchay, M. S. Seismic Processes and Migration of Magma  
739 during the Great Tolbachik Fissure Eruption of 1975–1976 and Tolbachik Fissure Eruption of 2012–  
740 2013, Kamchatka Peninsula. *Atmospheric and Oceanic Physics* 51 (7), 667–687 (2015).

- 741 73. Girina, O. A. Satellite high-resolution data used to clarify the position of fault zones within the  
742 Klyuchevskaya volcanic group of Kamchatka. *Sovremennye problemy distantsionnogo*  
743 *zondirovaniya Zemli iz kosmosa* 13, 148–156 (2016).
- 744 74. Mania, R., Walter, T. R., Belousova, M., Belousov, A. & Senyukov, S. L. Deformations and Morphology  
745 Changes Associated with the 2016–2017 Eruption Sequence at Bezymianny Volcano, Kamchatka.  
746 *Remote Sensing* 11, 1278 (2019).
- 747 75. Sulpizio, R., & Massaro, S., Influence of stress field changes on eruption initiation and dynamics: a  
748 review. *Frontiers in Earth Science* 5:18. (2017).
- 749 76. Coppola, D., Laiolo, M., Piscopo, D. & Cigolini, C. Rheological control on the radiant density of active  
750 lava flows and domes. *Journal of Volcanology and Geothermal Research* 249, 39–48 (2013).
- 751 77. Dai, C. & Howat, I.M. Measuring lava flows with ArticDEM: Application to the 2012-2013 eruption of  
752 Tolbachik, Kamchatka. *Geophysical Research Letters*, 44, 12133-12140 (2017).

753

754

## 755 **Acknowledgments**

756 This research was funded by the Italian Ministry for Universities and Research (MIUR). Part of this study was  
757 supported by the European Research Council under the European Union Horizon 2020 research and  
758 innovation program (Grant Agreement 787399-SEISMAZE) and by the Russian Ministry of Education and  
759 Science (Grant 14.W03.31.0033). We acknowledge the LANCE-MODIS system  
760 (<http://lancemodis.eosdis.nasa.gov/>) for providing Level 1B MODIS data.

761

## 762 **Author Contributions**

763 D.C. designed the study and conducted the analysis. M.L. and F.M. contributed to the analysis of MODIS data.  
764 N.S. provided the seismic data. S.H. conducted the statistical analysis. A.S., R.M., and T. W. reconstructed the  
765 eruptive history of volcanoes and interpreted satellite data in the light of independent observations. The  
766 ideas in the manuscript were developed through group discussions and written up principally by D.C. with  
767 contributions from all authors.

768

## 769 **Additional Information**

770 Supplementary information accompanies this paper:

771 (1) *Supplementary\_Material\_KVG\_Coppola.doc*;

772 (2) *Supplementary\_TableS1.xls*

773

## 774 **Competing Interests**

775 The authors declare no competing interests.